CHALMERS

Active noise control of an induction furnace

Thesis for the Master's Programme in Sound and Vibration

Karl Tillberg

Department of Civil and Environmental Engineering
Division of Applied Acoustics
CHALMERS UNIVERSITY OF TECHNOLOGY

MASTER'S THESIS 2006:41

Active noise control of an induction furnace

Karl Tillberg

Department of Civil and Environmental Engineering
Division of Applied Acoustics
CHALMERS UNIVERSITY OF TECHNOLOGY
Göteborg, Sweden 2006

Active noise control of an induction furnace

Master's Thesis 2006:41

Department of Civil and Environmental Engineering
Division of Applied Acoustics
Chalmers University of Technology
SE-41296 Göteborg
Sweden

Tel. +46-(0)31 772 1000

Reproservice / Department of Civil and Environmental Engineering
Göteborg, Sweden 2006

Active noise control of an induction furnce
Master's Thesis in the Master's programme in Sound and Vibration
Karl Tillberg
Department of Civil and Environmental Engineering
Division of Applied Acoustics
Chalmers University of Technology

Abstract

Induction furnaces are used to melt metals in the heavy industry. The noise from induction furnaces has always been a big problem. One of them is that the noise is tonal. This will result in that for quite low sound levels the noise can be very wearing, if you are exposed during long periods. But it is in the same time the tonality of the noise that makes it possible to get good results with active control. The goal with this thesis is to examine if the noise from an induction furnace can be controlled by active control. Things that have been done in this thesis are:

- An intensity measurement on the induction furnace at Scania foundary. The goal was to see if some parts of the furnace radiated more than others.
- Limiting the thesis by only looking at the part of the furnace that radiates most noise. The work has been done both theoretically and theoretically.
- In the theoretical part it was examined if active control was possible to use on this type of part. In the practical part a special speaker was built that should correspond to the sound field from the furnaces part. Then several control speakers was implemented to minimize the radiated sound from this model.

With this experiment setup a reduction of 25dB can be achieved theoretically for frequencies around 400Hz. In the pratical experiment different frequencies and types of sound radiation from the model was examined. For those a reduction of 5-13dB was achived.

Keywords: Induction furnace, Active noise control, XLMS algorithm.

Active noise control of an induction furnce
Master's Thesis in the Master's programme in Sound and Vibration
Karl Tillberg
Department of Civil and Environmental Engineering
Division of Applied Acoustics
Chalmers University of Technology

Sammanfattning

Induktionsugnar används till att smälta metall i den tunga industrin. Ljudet från induktionsugnar har alltid varit ett stort problem bland annat för att ljudet är tonalt. Detta medför att även för ganska låga ljudnivåer kan ljudet vara mycket påfrestande att utsättas för under långa perioder. Det är också på grund av att ljudet är tonalt som aktiv kontroll kan ge ett bra resultat.
Målet med detta arbete är att undersöka om ljudet från induktionsugnar kan kontrolleras med hjälp av aktiv kontroll. Det som har gjorts i detta examensarbete är i korta drag:

- En intensitetsmätning av induktionsugnen på Scania gjuteri. Detta för att se om vissa delar låter mer än andra.
- Från intensitetsmätningen har arbetet begränsats genom att enbart titta på den del av ugnen som låter mest. Arbetet har genomförts både teoretiskt och praktiskt.
- I den teoretiska delen har det undersökts om det är möjligt med aktiv kontroll på denna del. I den praktiska delen har en specialhögtalare byggts som ska motsvara ljudet från denna del. Sedan infördes så kallade kontrollhögtalare vars uppgift var att minska det utstrålade ljudet från modellen.

Med den uppsättning som experimentet har ska teoretiskt sett en reduktion på 25dB av den totala ljudeffekten kunna uppnås. Detta gäller för frekvenser runt 400Hz. I det praktiska experimentet undersöktes olika frekvenser och olika typer av ljudutstrålningar från modellen. För dessa uppnådes en reduktion mellan 5-13dB.

Nyckelord: Induktionsugn, Aktiv ljudkontroll, XLMS algoritm

Preface

This Master's Thesis has been made in cooperation with Ingemansson Technology AB, Göteborg and the department of Applied Acoustics at Chalmers University of Technology, Göteborg.

Acknowledgments

I would like to thank

- Wolfgang Kropp, my supervisor at Chalmers University of Technology.
- Martin Almgren, my supervisor at Ingemansson Technology AB.
- Peter Bengtsson, at Ingemansson Technology AB for the help with the intensity measurement.
- Börje Wijk, at Chalmers University of Technology for all help with the parts for the experiment.
- Thomas Beckman, for the help with the illustrations of the speaker.

Göteborg, May 18, 2006

Karl Tillberg

CONTENTS

1 INTRODUCTION

When you are melting scrap of metal in the heavy industry an induction furnace is often used. One problem with induction furnaces is that when they are in production they radiates noise. The goal of this thesis is to find out what kind of noise the furnace radiate, if the sound can be reduced with active control.

1.1 Background

1.1.1 What is an induction furnace?

An induction furnace uses magnetic field to melt metals. The principle of this melting technique is in general: if a conductor (the material that is heated) is placed in a magnetic field, eddy currents will be induced in the conductor and since every material has a resistance these currents will heat up the material.

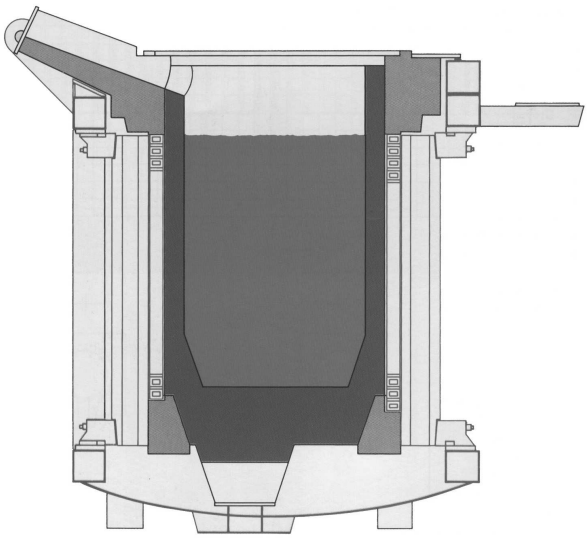

Figure 1.1. A section of an induction furnace.

This magnetic field is produced by a big electrical coil that surrounds the metals that is going to be melt. This coil is in most cases water cooled. It is this magnetic field that is the main source to the noise. Except the coil an induction furnace also has in general: a crucible (degel), magnetic yokes (plåtpaket) (this protects the surroundings from the magnetic field), exterior covering, a steel platform (where the furnace is hanging on and form a floor around the furnace), an electrical system (it is this system that is feeding the electrical coil).
How can a magnetic field be the main source of all the noise? The magnetic field

will cause forces on the material in the magnetic field called Lorenz forces. The connection between these forces and the magnetic field strength is:

$$F = \frac{1}{2}\mu H^2 \tag{1.1}$$

where F = force, H = magnetic field, μ = constant
This connection says that the force is proportional to the square of the magnetic field, and this will result in that the force will have the double frequency than the magnetic field. It is these forces that start parts of the furnace to vibrate and it is these vibrations that will radiate noise. I think that the magnetic yokes, the coil and the material, that is to be melting down, will be the biggest sound radiators.
How will the character of the sound be? Because the sound radiation is coming from magnetic field that is changing with just a pure frequency, the sound will also be a pure tone, but with the double frequency of the magnetic field. There will probably be some overtones. What frequency the furnace is fed with depends on what type of electronic the furnace has. For new furnaces the electronics that is used is with tyristors, and then the frequency is around 200 Hz. So the frequency of the acoustic noise will be around 400 Hz. For old furnaces they have some kind of mechanical rotors instead of the tyristors. For this "old" furnaces the frequency is around 500 Hz, which will create acoustic noise with a frequency around 1 kHz.

Figure 1.2. An induction furnace in industry.

(*Elektrougnar och induktiva omrörare* 1969), (D. H McQueen 1981), (McQueen 1982*a*), (McQueen 1982*b*)

1.1.2 Measurement of an induction furnace

In the end of June 2005 I was together with Peter Bengtsson on Ingemansson technology at SCANIA foundry in Södertälje to make some measurements on their new induction furnace.

Aim of measurement

The goal with this measurement was to see if some parts of the furnace radiate more sound than others. This was done by an intensity measurement, where the sound power radiation of different surfaces could be found. Apart from the intensity measurement the sound pressure level and some vibration measurements where measured at different places in the industry. The sound pressure where also recorded, this to get the frequency characteristics of the sound.

Results

Here are the measured A-weighted sound powers from main surfaces of the furnace.

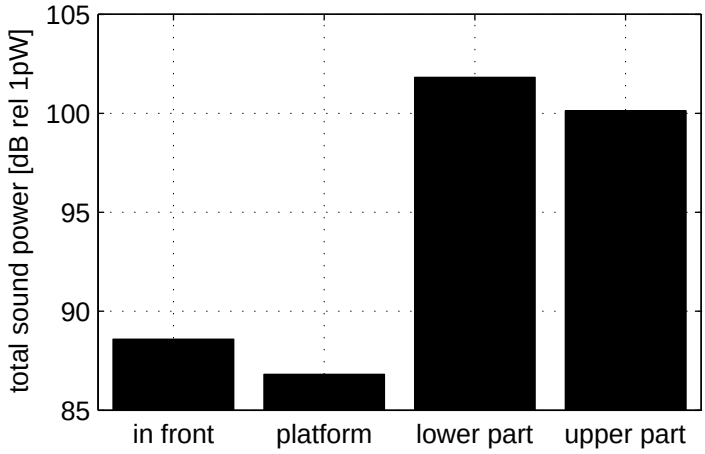

Figure 1.3. Sound power from main parts of the furnace.

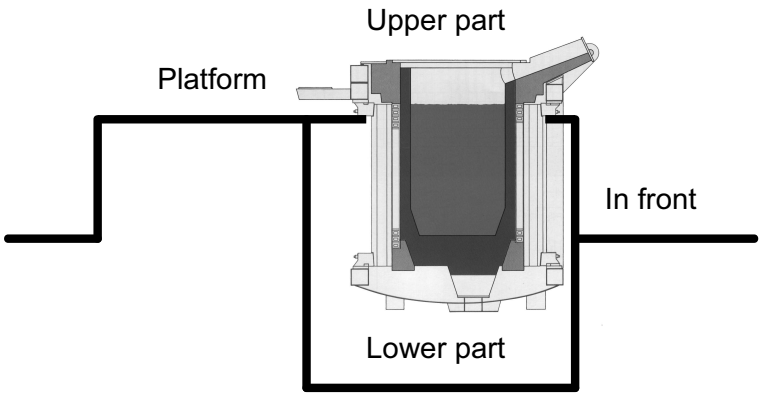

Figure 1.4. Illustration of main parts of the furnace.

In Figure 1.5 and Figure 1.6 there is a more detailed sound intesity measurement of the upper part of the furnace. Now the upper part is splited in small surfaces (see Figure 1.6) where the sound power is measured.

(*Determination of sound power levels of noise sources using sound intensity* 1996), (Fahy 1989)

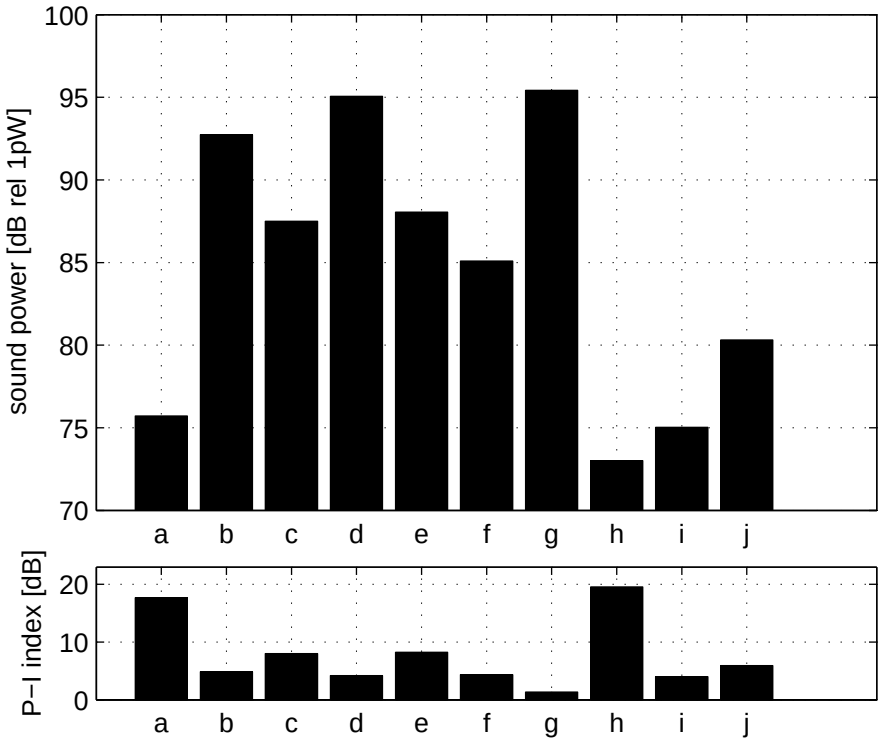

Figure 1.5. Sound power from upper parts of the furnace.

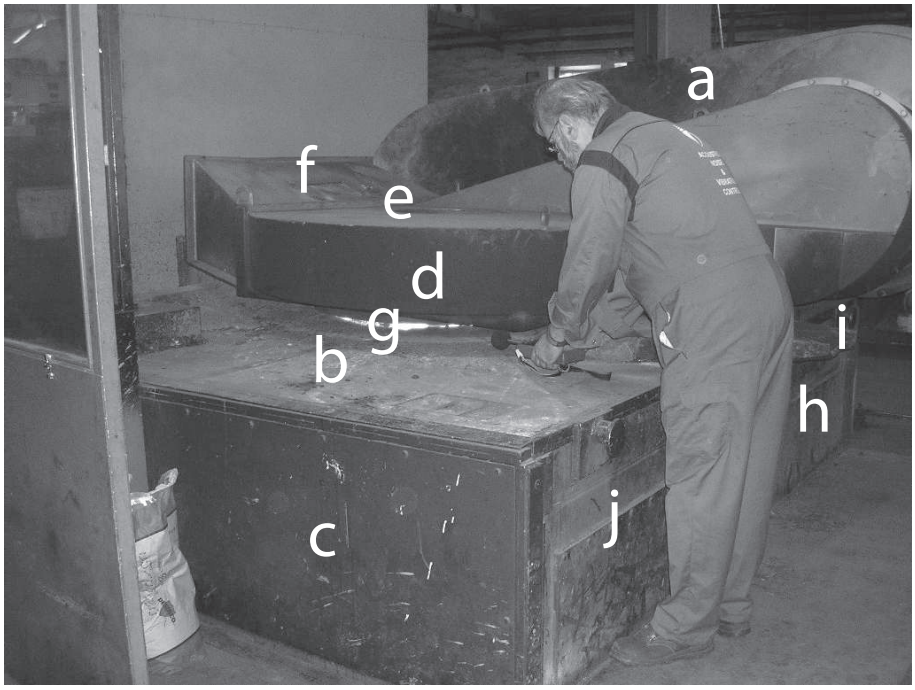

Figure 1.6. Part division of upper part.

In Figure 1.7 the power spectrum density (PSD) is is presented in 10 minutes interval for the time the furnace was running. (Hayes 1996)

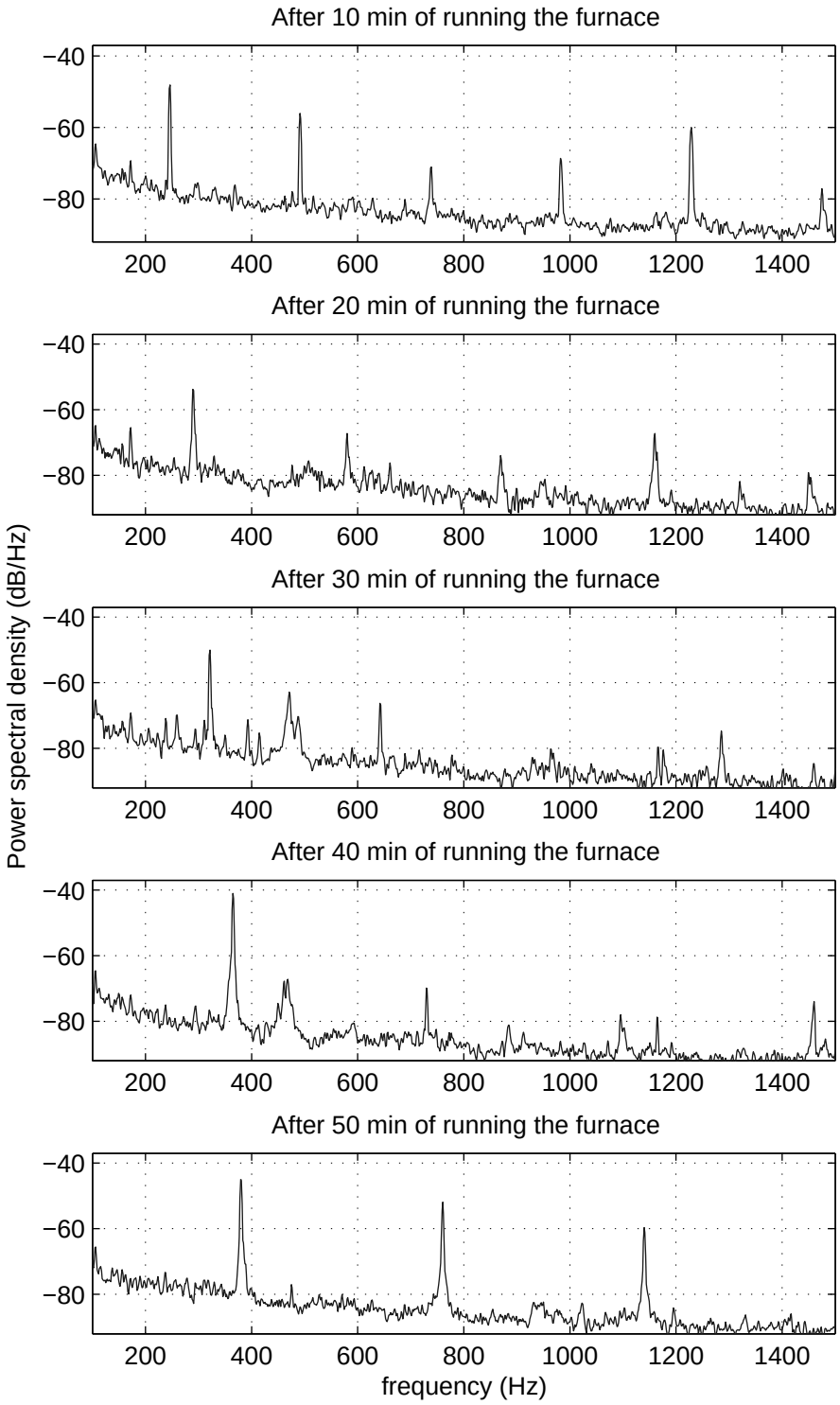

Figure 1.7. PSD for the furnace at different times.

Discussion

From the total sound power plot (Figure 1.3) it can be seen that the major part of the sound is coming directly from the furnace. The lower and upper parts are

both radiating much sound, but the lower part is inside a room of big concrete walls. The connection to the "outside" (from an acoustic point of view) from this room is only a surface that is included in the platform part in Figure 1.3, and from the platform is does not radiate much sound. Therefore the conclusion from this intensity measurement is that the top of the furnace is the part of the furnace that radiates most of the noise to the surroundings.
From the power spectrum density plots (Figure 1.7) can it be seen that the noise from the furnace is tonal. The fundamental frequency is almost 10 dB louder than the overtones, but some of the overtones is that high that they contributes to the total radiated sound. Therefore to get a god reduction of the noise the main thing is to focus on the fundamental frequency, but also to control some of the overtones. It can also be seen that the frequency is changed in time, at the beginning of the melting process the fundamental frequency is around 250Hz and at the end the frequency is almost 400Hz. Why this frequency is changed is since the frequency of the noise will be changed when the frequency of the magnetic field in the furnace is changed.

1.1.3 What is active control?

Active control essentially tries to eliminate sound or vibration components by adding the exact opposite sound or vibration. How this is done can be easily seen using two simple examples.

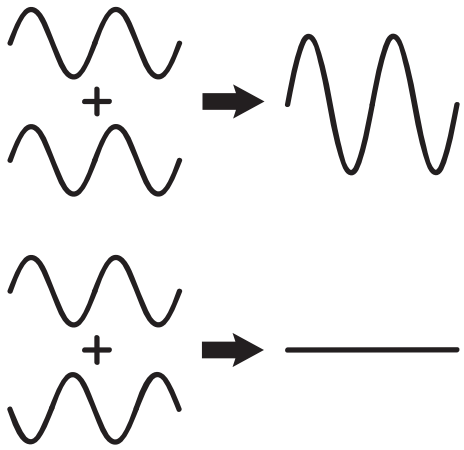

Figure 1.8. Two wawes with identical phase, and two waves with opposite phase.

The phase describes the relative position of the wave in its rising and falling cycle. If two waves are in phase, they rise and fall together, that will result in if they are exactly out out phase, one rises the other falls, and so they cancel out.
Why you can use this summation of two sound waves is that the sound is assumed to be linear (which allow us to superpose/add sounds).
One problem with active control is how to create this opposite sound field. First of all the sound/vibration signal (called reference signal) must be measured some where, this to get the character of the sound (if it's broadband, tonal, frequency range etc.). This can be done for instance by placing a microphone (called detection mic) in the sound field. If the sound/vibration is coming from a machine that having rotating parts the reference signal can be found from the rotation of the machine by a tachometer. When the reference signal is found it must then be shifted in time and amplified so it fits the sound/vibration as Figure 1.8. This phase shift and amplification is usually done by a digital signal processor (DSP).
(Snyder 2000), (P.A. Nelson 1992)

1.1.4 Why active control on an induction furnace?

The most of the noise from an induction furnace is coming from the opening between the furnace and the lid (see section 1.1.2). This opening can not be closed and it radiates a lot of heat which is why it is difficult to use passive control here. The alternative to this is active control and this can probably work in this situation.
Other reasons why active control may work are:
The noise from an induction furnace is tonal, which is why you can get good results

with active control. The reference signal can be found from the magnetic field, that will result in no need of a detection microphone. Active control does not take a lot of space, because when this furnace is in production it must be loaded, unloaded, take samples from the melt etc., which results in that it complicates the work if the furnace is for instance build in a free-standing house.
Is there anything that can be a problem with active control?
This type of furnaces has dimensions that is around the size of the wavelength. There is also probably lot of parts that radiates from the furnace, and this will result in a complex sound field.

1.2 Previous work

In 1981-82 Douglas McQueen published in Scandinavian journal (D. H McQueen 1981), (McQueen 1982*a*), (McQueen 1982*b*) three articles on reduction of noise from induction furnaces. His suggestion of noise reduction was roughly to enclose the furnace with a house with absorbers on the walls. In his investigation he started with

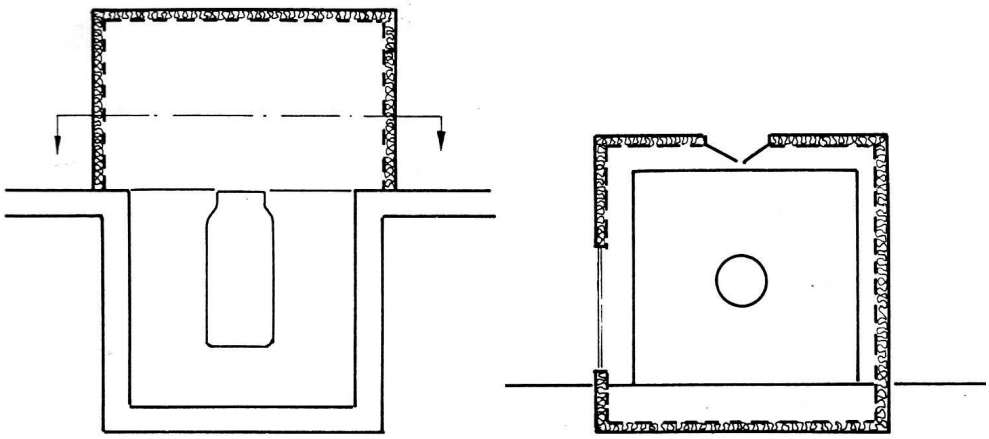

Figure 1.9. McQueens House.

measuring the sound pressure level on three different furnaces. Then he made a simple model of the furnace, where he assumed that the vibrations that created the sound field only come from the magnetic yokes. The vibrations was then transmitted to all parts of the furnace, and from this model and measurements on furnaces he made the "house conclusion".
In 1994 ABB published an article (Dötsch 1994) where they described how they could make inductions furnaces quieter. In the article they focused on the vibrations from the electric coil. The vibrations in the coil are both radial- and axial. Their solution to get rid of the vibrations was to fasten the coil so hard they could in both radial and axial directions. In axial direction the coil was fasten with concrete rings, concrete for the good damping effects so no stucture born sound could appear. For the radial vibrations they designed a new magnetic yoke (see Figure 1.10). This

new yoke have a very god damping effect and high eigen frequency.

In 1999-2001 a group in Germany made a numerical 3D model of an induction

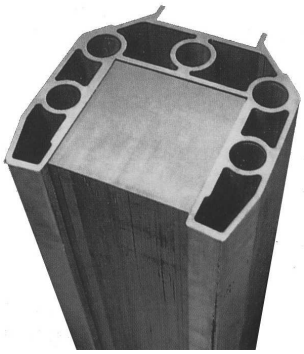

Figure 1.10. Picture of ABB's new yokes.

furnace (see Figure 1.11). They published this in three articles (T. Bauer 1999), (T. Bauer 2000), (T. Bauer 2001). In the first one the model was created, in the second an improved model of the furnaces was created. In the last article they compared the model to a experimental modal analysis of an induction furnace and to acoustic measurements in normal operating mode. The conclusion in this series of article they write: *This contribution presents an improved coupled 3D noise calculation. A comparison of the mode shapes and the sound field of the induction furnace shows good correspondence and proofs the method to be a suitable tool for further investigation in order to reduce the sound emission of induction furnaces and other electrical machines.*

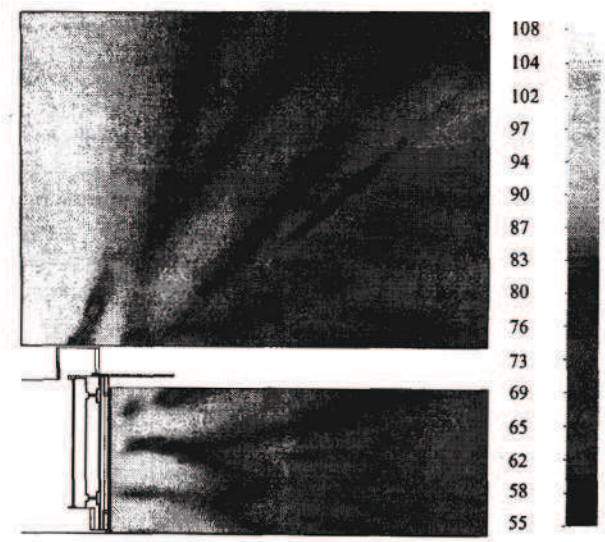

Figure 1.11. FEM model of an induction furnace.

2 THESIS FRAMEWORK

From the intensity measurement in section 1.1.2 it can be seen that the little opening between the furnace and the lid radiates most noise (about 6dB more than other parts). Therefore instead of examine the sound field from the complete furnace (that is very complex), this thesis will examine the sound field from this thin opening called a slit (see Figure 2.1). The goal with this thesis is to reduce the noise from this slit by active controll, and why active controll is because this opening never can be closed and it is hard to reduce the noise passive, since the temperature is so high.

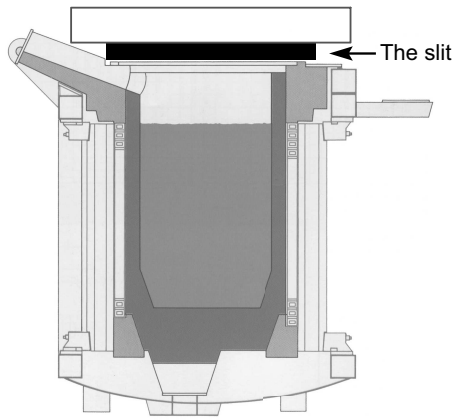

Figure 2.1. The slit part of the induction furnace.

2.1 Assumptions

To simplify the problem the slit is assumed to be straight insted of round (see Figure 2.2). The noise from the slit is assumed to be tonal with one frequency (no

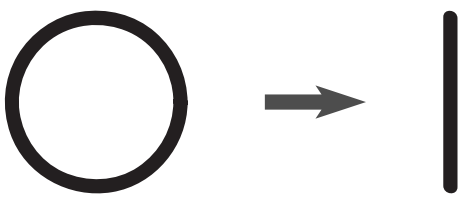

Figure 2.2. From a round slit to a straigth slit.

overtones) and stationary (it will not change in time). The length of the slit will be be 0.7 wavelengths, and for a frequency of 400Hz will give a length of the slit of 0.6m.

2.2 Aim of thesis

The aim of this thesis is to examine the noise from the slit part of the furnace. This is done by building a speaker that radiate noise from a slit, where the noise shall create the same sound field as the slit part of the furnace. The sound field from the speaker shall be able to be changed in some different ways (see Figure 2.3), where different ways means that the particle velocity in the slit is changed. Different ways since we don't know exactly how the sound field from the opening of the furnace is.

This sound field from our new model of the furnace will then be reduced by an

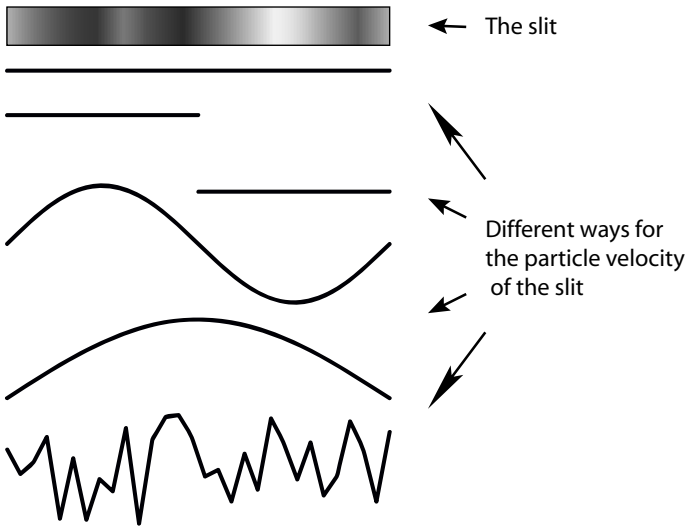

Figure 2.3. Ideas for different particle velocities for the slit.

active noise control system that has some secondary sources. A problem with the placement of secondary sources is that it is hard to place those near the slit. Thus for a real furnace it gets very hot, and this will probably result in broken speakers. The idea is therefore to lead the sound from the driver/speaker by a rigid tube to the slit, so the drivers can be placed some distance away from the slit. This idea of secondary sources can be seen in Figure 2.4.

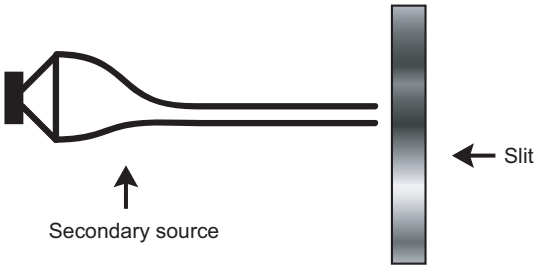

Figure 2.4. Idea for secondary sources.

2.3 Structure of thesis

To examine this implementation of an active control system on the slit the work is done in several steps. They are presented shortly following.
The first thing to do is to see theoretical how much reduction of the sound radiation that can be achieved by adding some secondary sources, where the goal is to minimize total radiated sound power. In this part it will also be examined where it is best to place the secondary sources, and how much better reduction there will be by including more secondary sources. In this first theoretical part the wave equation is solved in the frequency domain, and the secondary sources are assumed to be point sources. This is done in section 3.1.
The next step that is done is the problem on how to measure the total power. This is done in section 3.2.
After we know where and how many secondary sources that is going to be used and how to measure radiated sound power the question on how to controll the secondary sources is examined. The idea is to use the feed forward multichannel XLMS algorithm and is done in section 3.3.
After the theory parts the the slit speaker and secondary sources for the experiment will be build, controlled and placed in the experiment, and the entire experiment is presented in chapter 4.
For the experiment the XLMS-algorithm can be used either in real time or be pre processed by the time domain model. Real time would be the best solution, the filter will adapt itself if some parts of the system is changed and the exact transfer functions of the slit path will be used. A problem with this is that you must have electronics that can handle systems with multiple input and output signals in real time. The department of acoustics only have two in two out DSP cards. Therefore for this thesis the preprocessed approach will be used. The preprocessed approach is shortly like this:

- Measure all transfer paths (slit paths, secondary paths)
- From this measurement describe the transfer paths as FIR filters (make models of the transfer paths)
- Import these models in the time simulation model
- From the model the filter coefficients is found
- Import the filter coefficients in the real experiment and see if it works as expected

In chapter 5 the results from the experiment is shown, and followed by a discussion in chapter 6 and at last a final conclusion for the thesis, which is in in chapter 7.

3 THEORY

3.1 Simulations in the frequency domain

The goal with this theory part is to examine of what is happening with the total sound power if the placement and the number of secondary sources is changed. The first thing that is done is the formulation of the sound pressure from a point source. This point source will then be used in section 3.1.2 and 3.1.3. In section 3.1.2 the slit is described as one point source in a baffle that is controlled by one point source as secondary source. In section 3.1.3 the model of the slit is described by N point sources in a baffle and is then controlled by M point sources as secondary sources.

3.1.1 Basics on a Monopole

To find a formulation of the sound pressure for a monopole the wave equation (Eq 3.1) is used.

$$c^2 \nabla^2 p - \frac{\partial^2 p}{\partial t^2} = 0 \tag{3.1}$$

For spherical coordinates (r, φ, ϑ) the wave equation has the general sollution if you assume a harmonic wave.

$$p\left(r,t\right) = \frac{A}{r} e^{j(\omega t - kr)} + \frac{B}{r} e^{j(\omega t + kr)} \tag{3.2}$$

Equation (3.2) says that there is one wave in and one out. By only looking at the wave out, the sound pressure will look like Eq (3.3).

$$p\left(r,t\right) = \frac{A}{r} e^{j(\omega t - kr)} \tag{3.3}$$

The equation of motion for gases is

$$-\frac{\partial p}{\partial r} = \rho_0 \frac{\partial v}{\partial t} \tag{3.4}$$

were ρ_0 is the density of air, v is the particle velocity.

Inserting Eq (3.4) in Eq (3.3) will give this.

$$\begin{aligned}\frac{\partial v(t,r)}{\partial t} &= -\frac{1}{\rho_0}(-\frac{A}{r^2}e^{j(\omega t-kr)} + \frac{(-)jkA}{r}e^{j(\omega t-kr)}) = \\ = \frac{A}{\rho_0}(\frac{1}{r^2} + \frac{jk}{r})e^{j(\omega t-kr)} &= \frac{A}{\rho_0 r}jk(1+\frac{1}{jkr})e^{j(\omega t-kr)} = \\ &= \frac{Aj\omega}{\rho_0 cr}(1+\frac{1}{jkr})e^{j(\omega t-kr)} \end{aligned} \tag{3.5}$$

To get rid of the time derivation, the expression in Eq (3.5) will be formaulated in the frequency domain.

$$\frac{\partial v(t,r)}{\partial t} = j\omega v(\omega,r) \;\Rightarrow\; v(\omega,r) = \frac{A}{\rho_0 cr}(1+\frac{1}{jkr})e^{j(\omega t-kr)} \tag{3.6}$$

Now there is an expression for the sound pressure and particle velocity in spherical cordinates. To find a value of the A variable there must be some boundary conditions (BC). Assume a sphere with radius a and volum flow q (velocity of sphere v is $v = \frac{q}{4\pi a^2}$). Now the point source will be a volume flow source.

$$\text{Boundary Condition: } v(r=a,\,\omega) = \frac{q}{4\pi a^2}e^{j\omega t} \tag{3.7}$$

Inserting the BC on Eq (3.6) will give an expression for A (Eq 3.8).

$$\begin{aligned}\frac{q}{4\pi a^2}e^{j\omega t} = v(r=a,\omega) &= \frac{A}{\rho_0 ca}(1+\frac{1}{jka})e^{j(\omega t-ka)} \\ \frac{q}{4\pi a^2} = \frac{A}{j\omega\rho_0 a^2}(1+jka)e^{-jka} &\;\Rightarrow\; A = \frac{j\omega\rho_0}{4\pi}\frac{q}{1+jka}e^{jka}\end{aligned} \tag{3.8}$$

Inserting A in Eq (3.3) will give a final expression for the sound pressure from a point source.

$$\begin{aligned}p(r) &= \frac{j\omega\rho_0}{4\pi r}\frac{q}{1+jka}e^{j(\omega t-k(r-a))} \\ if\ a\to 0 \;&\Rightarrow p(r) = \frac{j\omega\rho_0 q}{4\pi r}e^{j(\omega t-kr)}\end{aligned} \tag{3.9}$$

Equation (3.9) is the final formulation for the sound pressure from a point source, and this will be used in sections 3.1.2 and 3.1.3 to the formulation of the sound pressure from a slit.

(Kleiner 1991)

3.1.2 Active controll of one point source in a baffle with one secondary source

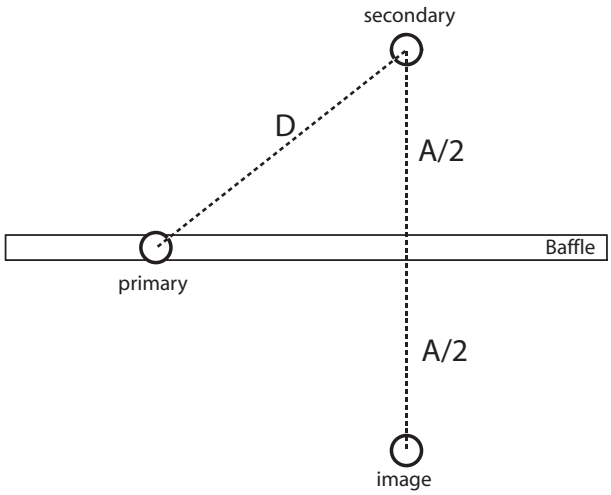

Figure 3.1. Point source in baffle with one secondary source.

The goal with this part is to examine analytical on what happens when the secondary sources is placed on different places when the goal is to minimize the total sound power. This is for a point source in a baffle when it is controlled by a point source above the baffle. The fact that the baffle is included an image source from the secondary source will be included (see Figure 3.1). The volume flow for the secondary source will be changed (is the variable) and the volume flow for the primary source will be constant (is the boundary condition). The point sources has volume flows q_p and q_s ($_p$ as primary, $_s$ as secondary). The first step by formulating the total power is to formulate the sound power for each point source.The total sound power is then the sum of all powers ($W_{tot} = W_p + W_s + W_i$). To get the sound power from each source the total sound pressure in each point need to be found. This since the sound power contribution from each source are: $W = \frac{1}{2}Re(p \cdot q)$, where p is the total sound pressure in that point and q is the volume flow for that point. The total sound pressure $p(\mathbf{r})$ in a point $\mathbf{r}$ is:

$$\begin{aligned} p(\mathbf{r}) &= p_p(\mathbf{r}) + p_s(\mathbf{r}) + p_i(\mathbf{r}) \\ p_p &= \text{sound pressure from primary source} \\ p_s &= \text{sound pressure from secondary source} \\ p_i &= \text{sound pressure from image source} \end{aligned} \tag{3.10}$$

The pressure from the different sources at point $\mathbf{r}$ are

$$\begin{aligned} p_p(\mathbf{r}) &= \frac{j\omega\rho_0 q_p}{2\pi\left|\mathbf{r}-\mathbf{p}\right|} e^{j(\omega t - k|\mathbf{r}-\mathbf{p}|)} \\ p_s(\mathbf{r}) &= \frac{j\omega\rho_0 q_s}{4\pi\left|\mathbf{r}-\mathbf{s}\right|} e^{j(\omega t - k|\mathbf{r}-\mathbf{s}|)} \\ p_i(\mathbf{r}) &= \frac{j\omega\rho_0 q_s}{4\pi\left|\mathbf{r}-\mathbf{i}\right|} e^{j(\omega t - k|\mathbf{r}-\mathbf{i}|)} \end{aligned} \tag{3.11}$$

where $\mathbf{p}$, $\mathbf{s}$, $\mathbf{i}$ is the placement of primary-, secondary- and image source. The pressure from the primary source differs from secondary source by a factor of two. This because that the primary source is mounted on a baffle and it is radiating only outward the baffle. The total power from primary source can then be described like Eq (3.12).

$$\begin{aligned} W_p &= \frac{1}{2} Re\{(p_p + p_s + p_i)^*\, q_p\} = \\ &= \frac{1}{2} Re\{p_p^*\, q_p\} + \frac{1}{2} Re\{p_s^*\, q_p\} + \frac{1}{2} Re\{p_i^*\, q_p\} \end{aligned} \tag{3.12}$$

$$\begin{aligned} \frac{1}{2} Re\{p_p^*\, q_p\} &= \frac{1}{2} \frac{\omega\rho_0 q_p^*\, q_p k}{2\pi} Re\{\frac{j e^{-jk|\mathbf{p}-\mathbf{p}|}}{k\left|\mathbf{p}-\mathbf{p}\right|}\} = \\ \frac{1}{2} \frac{\omega\rho_0 q_p^*\, q_p k}{2\pi} \frac{1}{k\left|\mathbf{p}-\mathbf{p}\right|} Re\{j\cos(k\left|\mathbf{p}-\mathbf{p}\right|) + \sin(k\left|\mathbf{p}-\mathbf{p}\right|)\} &= \\ = \frac{1}{2} \frac{\omega\rho_0 q_p^*\, q_p\, k}{2\pi} \frac{\sin(k\left|\mathbf{p}-\mathbf{p}\right|)}{k\left|\mathbf{p}-\mathbf{p}\right|} = \frac{1}{2} \frac{\omega\rho_0 k}{2\pi} \left|q_p\right|^2 &= \\ = (z_o = \frac{\omega\rho_0 k}{4\pi}) = z_0 \left|q_p\right|^2 \end{aligned} \tag{3.13}$$

In similar way as Eq (3.13) $\frac{1}{2} Re\{p_s^*\, q_p\}$ and $\frac{1}{2} Re\{p_i^*\, q_p\}$ is formulated

$$\frac{1}{2} Re\{p_s^* q_p\} = \frac{z_0}{2} \frac{\sin(k\left|\mathbf{p}-\mathbf{s}\right|)}{k\left|\mathbf{p}-\mathbf{s}\right|} q_p\, q_s^* \tag{3.14}$$

$$\frac{1}{2}Re\{p_i^* q_p\} = \frac{z_0}{2}\frac{\sin(k\,|\mathbf{p}-\mathbf{i}|)}{k\,|\mathbf{p}-\mathbf{i}|} q_p\, q_s^* \tag{3.15}$$

Since the distance between primary and secondary source ($|\mathbf{p}-\mathbf{s}|$) and primary and image source ($|\mathbf{p}-\mathbf{i}|$) are the same, the power from these are same. So inserting Eq (3.13), (3.14), (3.15) in Eq (3.12) will give a final expresson for W_p. In Eq (3.16) the distance $|\mathbf{p}-\mathbf{s}|$ is defined as D.

$$W_p = z_o(|q_p|^2 + \frac{\sin(kD)}{kD} q_p\, q_s^*) \tag{3.16}$$

The powers from the secondary- and the image source can be formulated in the same way as the power from the primary source. The systems geometry (see Figure 3.1) also results in the same powers from the secondary- and the image source. This power can be described like Eq (3.17).

$$W_s = W_i = \frac{1}{2} z_o(|q_s|^2 \; + 2q_p^* q_s \frac{\sin(kD)}{kD} + |q_s|^2 \frac{\sin(kA)}{kA}) \tag{3.17}$$

In Eq (3.17) is A is the distance between the secondary and the image source (see Figure 3.1). The total power can now be formulated.

$$\begin{aligned} W_{tot} &= W_p + W_s + W_i = \\ &= z_o(|q_p|^2 + \frac{\sin(kD)}{kD} q_p\, q_s^* + |q_s|^2 \; + 2q_p^*\, q_s \frac{\sin(kD)}{kD} + |q_s|^2 \frac{\sin(kA)}{kA}) = \\ &\qquad z_o(|q_p|^2 + |q_s|^2 (1 + \frac{\sin(kA)}{kA}) + (q_p\, q_s^* + 2q_p^*\, q_s)\frac{\sin(kD)}{kD}) \end{aligned} \tag{3.18}$$

$$def. \;\; H(j\omega) = \frac{q_s}{q_p} \;\Rightarrow\; q_s = q_p\, H(j\omega) \tag{3.19}$$

Inserting Eq (3.19) in Eq (3.18) the total sound power is descibed like this.

$$W_{tot} = z_o\,|q_p|^2 (1 + |H|^2 (1 + \frac{\sin(kA)}{kA}) + (H^* + 2H)\frac{\sin(kD)}{kD}) \tag{3.20}$$

Since H is a complex quantity, it can therefore be defined as Eq (3.21).

$$def. \;\; H = a + jb \tag{3.21}$$

$$W_{tot} \;=\; z_o\,|q_p|^2\,\{1 \;+\; (a^2 \;+\; b^2)(1 \;+\; \frac{\sin(kA)}{kA}) \;+\; +(3a \;+\; jb)\frac{\sin(kD)}{kD}\} \quad (3.22)$$

Eq (3.22) is a quadratic function, and therefore to get the minimum of the power (W_{min}) (3.22) is derived with respect to a and b and set equal to zero.

$$\frac{\partial W_{tot}}{\partial a} = z_o\,|q_p|^2\,(2a + 2a\frac{\sin(kA)}{kA}) + 3\frac{\sin(kD)}{kD}) = 0$$
$$\Rightarrow\; a(1 + \frac{\sin(kA)}{kA}) = -\frac{3}{2}\frac{\sin(kD)}{kD} \Rightarrow\; a = -\frac{3}{2}\frac{\frac{\sin(kD)}{kD}}{1 + \frac{\sin(kA)}{kA}} \quad (3.23)$$

$$\frac{\partial W_{tot}}{\partial b} = z_o\,|q_p|^2\,(2b + 2b\frac{\sin(kA)}{kA}) + j\frac{\sin(kD)}{kD}) = 0 \Rightarrow\; b = -\frac{j}{2}\frac{\frac{\sin(kD)}{kD}}{1 + \frac{\sin(kA)}{kA}} \quad (3.24)$$

$$\mathrm{sinc}(kA) = \frac{\sin(kA)}{kA}\;,\; \mathrm{sinc}(kD) = \frac{\sin(kD)}{kD} \quad (3.25)$$

Inserting Eq (3.23), (3.24), (3.25) in Eq (3.19) will give q_s.

$$q_s \;=\; -\;q_p(-\frac{3}{2}\frac{\mathrm{sinc}(kD)}{1 + \mathrm{sinc}(kA)} \;-\; \frac{j^2}{2}\frac{\mathrm{sinc}(kD)}{1 + \mathrm{sinc}(kA)}) \;=\; -\;q_p\frac{\mathrm{sinc}(kD)}{1 + \mathrm{sinc}(kA)} \quad (3.26)$$

Inserting Eq (3.26) in Eq (3.18) will give the total minimun power (W_{min})

$$W_{min} = z_0\,|q_p|^2\,(1 + \frac{\mathrm{sinc}^2(kD)}{(1 + \mathrm{sinc}(kA))^2} - 3\frac{\mathrm{sinc}^2(kD)}{1 + \mathrm{sinc}(kA)} + \frac{\mathrm{sinc}^2(kD)\mathrm{sinc}(kA)}{(1 + \mathrm{sinc}(kA)^2})$$
$$W_{min} = z_0\,|q_p|^2\,\{1 - (3\frac{\mathrm{sinc}^2(kD)}{1 + \mathrm{sinc}(kA)} - \frac{\mathrm{sinc}^2(kD) + \mathrm{sinc}^2(kD)\mathrm{sinc}(kA)}{(1 + \mathrm{sinc}(kA))^2})\} \quad (3.27)$$

From Eq 3.27 can it be seen that the minumun of the total power is a function of the distance between primary and secondary source (D), and the distance beween the primary and image source (A, this distance is the same as twice the distance between secondary source and baffle in normal direction of baffle). To understand what Eq 3.27 says, it is presented in Figure 3.2 were the secondary source is placed at different places. Primary source is placed in origin.

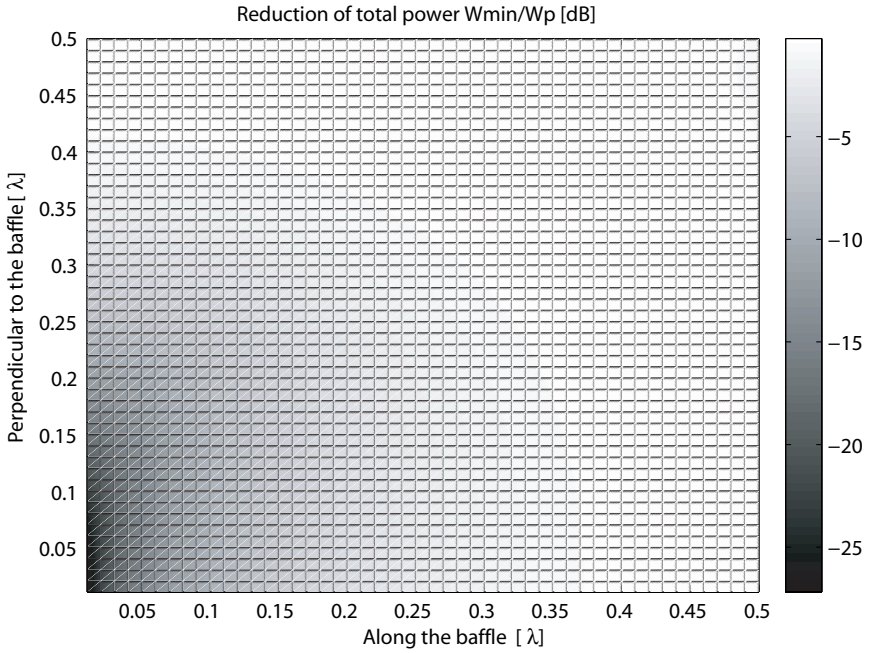

Figure 3.2. Reduction of the total power with 1 point source in baffle controlled by 1 secondary source at different places

From Figure 3.2 can it be seen that the closer secondary source is placed primary source, the better reduction of total power. It can also be seen that it is better to place secondary source above primary source than along the baffle. From Eq 3.27 and Figure 3.2 it can also be seen that secondary source must be placed closer than 0.5 wavelength from primary source to get any reduction. (P. A. Nelson 1987)

3.1.3 Active control of N point sources in a baffle with M secondary sources

The goal with this part is to formulate an expression where the number of secondary and primary point sources easily can be changed. To get the total power the sound power from all point sources must be formulated. The sound power for one source is defined as

$$W = \frac{1}{2} Re(p_{total}\, q^*) \tag{3.28}$$

where p_{total} is the total sound pressure from all present sources, q is the source strength from the source. Before including primary-, secondary- and image sources assume that there is N point sources. This so it can be formulated an general expression for the total power when there is many point sources. The strength of all sources can be specified by a complex vector $\mathbf{q}$, where

$$\mathbf{q}^{\mathrm{T}} = [\, q_1(\omega), q_2(\omega), \ldots, q_n(\omega), \ldots, q_N(\omega)\,] \tag{3.29}$$

such that $q_n(\omega)$ is the complex strength of the nth source and there are N sources in total. The pressures produced by these sources at each of the N source locations can be expressed as a complex vector $\mathbf{p}$. This can be related to the source strength vector via a matrix $\mathbf{Z}$ of complex impedances such that

$$\mathbf{p} = \mathbf{Z}\,\mathbf{q} \tag{3.30}$$

where the vector $\mathbf{p}$ of order N and matrix $\mathbf{Z}$ or order N x N are given by

$$\mathbf{p} = \begin{bmatrix} p\,(\mathbf{x}_1, \omega) \\ p\,(\mathbf{x}_2, \omega) \\ \vdots \\ p\,(\mathbf{x}_n, \omega) \\ \vdots \\ p\,(\mathbf{x}_N, \omega) \end{bmatrix}, \quad \mathbf{Z} = \begin{bmatrix} z_1\,(\mathbf{x}_1, \omega) & z_2\,(\mathbf{x}_1, \omega) \cdots z_n\,(\mathbf{x}_1, \omega) \cdots z_N\,(\mathbf{x}_1, \omega) \\ z_1\,(\mathbf{x}_2, \omega) & z_2\,(\mathbf{x}_2, \omega) \cdots z_n\,(\mathbf{x}_2, \omega) \cdots z_N\,(\mathbf{x}_2, \omega) \\ \vdots & \vdots \quad\quad \vdots \quad\quad \vdots \\ z_1\,(\mathbf{x}_n, \omega) & z_2\,(\mathbf{x}_n, \omega) \cdots z_n\,(\mathbf{x}_n, \omega) \cdots z_N\,(\mathbf{x}_n, \omega) \\ \vdots & \vdots \quad\quad \vdots \quad\quad \vdots \\ z_1\,(\mathbf{x}_N, \omega) & z_2\,(\mathbf{x}_N, \omega) \cdots z_n\,(\mathbf{x}_N, \omega) \cdots z_N\,(\mathbf{x}_N, \omega) \end{bmatrix} \tag{3.31}$$

The total power from the sources can now be written as

$$W = \frac{1}{2} Re(\mathbf{p}^{\mathrm{H}}\,\mathbf{q}) \tag{3.32}$$

Where H denotes the Hermitian transpose of the vector $\mathbf{p}$ which is the complex conjugate of $\mathbf{p}^{\mathrm{T}}$. Importing Eq (3.30) into Eq (3.32) will give the expression

$$W = \frac{1}{2} Re\{\mathbf{q}^{\mathrm{H}}\,\mathbf{Z}^{\mathrm{H}}\,\mathbf{q}\} = \frac{1}{2}\,\mathbf{q}^{\mathrm{H}} Re\{\mathbf{Z}^{\mathrm{H}}\}\,\mathbf{q} \tag{3.33}$$

Now when an expression of the total power for N point sources is formulated, there will be formulated an expression where the primary- and the secondary sources is separated.
The strength of all N primary sources can be specified by a complex vecktor $\mathbf{q}_p$, where

$$\mathbf{q}_p{}^{\mathrm{T}} = [q_1(\omega), q_2(\omega), ..., q_N(\omega)] \tag{3.34}$$

For all M secondary sources including the image sources the strength will be in a complex vecktor $\mathbf{q}_s$, where

$$\mathbf{q}_s{}^{\mathrm{T}} = [q_1(\omega), q_2(\omega), ..., q_{2M}(\omega)] \tag{3.35}$$

has a length of is $2M$ becasue that every secondary source will have an image source from the influence of the baffle. The vector of pressures produced on the primary sources by the primary sources will be specified by the complex vector $\mathbf{p}_p(\mathbf{x}_p)$, and the vector of pressures produced on the primary sources by the secondary sources will be specified by the complex vector $\mathbf{p}_s(\mathbf{x}_p)$, where $\mathbf{x}_p$ is a vector of the places for the primary sources. The power from the primary sources is then given by Eq (3.36).

$$W_{primary} = \frac{1}{2} Re\{[\,\mathbf{p}_p(\mathbf{x}_p) + \mathbf{p}_s(\mathbf{x}_p)\,]^{\mathrm{H}}\,\mathbf{q}_p\} \tag{3.36}$$

An exactly analogous argument can be applied to the calculation of the power output of secondary sources. Thus the pressure at the secondary sources preoduced by the secondary sources is $\mathbf{p}_s(\mathbf{x}_s)$ and the pressure at secondary sources produced by the primary sources is $\mathbf{p}_p(\mathbf{x}_s)$. The total power output of both secondary and primary souces can be written as Eq (3.37).

$$W_{total} = \frac{1}{2} Re\{[\,\mathbf{p}_s(\mathbf{x}_s) + \mathbf{p}_p(\mathbf{x}_s)\,]^{\mathrm{H}}\,\mathbf{q}_s + [\,\mathbf{p}_p(\mathbf{x}_p) + \mathbf{p}_s(\mathbf{x}_p)\,]^{\mathrm{H}}\,\mathbf{q}_p\} \tag{3.37}$$

The vectors of pressures can be related to source strength via impedance matrices such that $\mathbf{p}_s(\mathbf{x}_s) = \mathbf{Z}_s(\mathbf{x}_s)\,\mathbf{q}_s$, $\mathbf{p}_p(\mathbf{x}_s) = \mathbf{Z}_p(\mathbf{x}_s)\,\mathbf{q}_p$, $\mathbf{p}_p(\mathbf{x}_p) = \mathbf{Z}_p(\mathbf{x}_p)\,\mathbf{q}_p$, $\mathbf{p}_s(\mathbf{x}_p) = \mathbf{Z}_s(\mathbf{x}_p)\,\mathbf{q}_s$, where

$$\begin{aligned} &Re\{\mathbf{Z}_s(\mathbf{x}_s)\} = \\ &= z_o \begin{bmatrix} 1 & \mathrm{sinc}(k\,|\mathbf{x}_{s1} - \mathbf{x}_{s2}|) & \cdots & \mathrm{sinc}(k\,|\mathbf{x}_{s1} - \mathbf{x}_{s2M}|) \\ \mathrm{sinc}(k\,|\mathbf{x}_{s2} - \mathbf{x}_{s1}|) & 1 & \cdots & \mathrm{sinc}(k\,|\mathbf{x}_{s2} - \mathbf{x}_{s2M}|) \\ \vdots & \vdots & & \vdots \\ \mathrm{sinc}(k\,|\mathbf{x}_{s2M} - \mathbf{x}_{s1}|) & \mathrm{sinc}(k\,|\mathbf{x}_{s2m} - \mathbf{x}_{s2}|) & \cdots & 1 \end{bmatrix} \end{aligned} \tag{3.38}$$

$$\begin{aligned} &Re\{\mathbf{Z}_s(\mathbf{x}_p)\} = \\ &= z_o \begin{bmatrix} \mathrm{sinc}(k\,|\mathbf{x}_{p1} - \mathbf{x}_{s1}|) & \mathrm{sinc}(k\,|\mathbf{x}_{p1} - \mathbf{x}_{s2}|) & \cdots & \mathrm{sinc}(k\,|\mathbf{x}_{p1} - \mathbf{x}_{s2M}|) \\ \mathrm{sinc}(k\,|\mathbf{x}_{p2} - \mathbf{x}_{s1}|) & \mathrm{sinc}(k\,|\mathbf{x}_{p2} - \mathbf{x}_{s2}|) & \cdots & \mathrm{sinc}(k\,|\mathbf{x}_{p2} - \mathbf{x}_{s2M}|) \\ \vdots & \vdots & & \vdots \\ \mathrm{sinc}(k\,|\mathbf{x}_{pN} - \mathbf{x}_{s1}|) & \mathrm{sinc}(k\,|\mathbf{x}_{pN} - \mathbf{x}_{s2}|) & \cdots & \mathrm{sinc}(k\,|\mathbf{x}_{pN} - \mathbf{x}_{s2M}|) \end{bmatrix} \end{aligned} \tag{3.39}$$

$$Re\{\mathbf{Z}_p(\mathbf{x}_p)\} = \\ = z_o \begin{bmatrix} 1 & \operatorname{sinc}(k\,|\mathbf{x}_{p1}-\mathbf{x}_{p2}|) & \cdots & \operatorname{sinc}(k\,|\mathbf{x}_{p1}-\mathbf{x}_{pN}|) \\ \operatorname{sinc}(k\,|\mathbf{x}_{p2}-\mathbf{x}_{p1}|) & 1 & \cdots & \operatorname{sinc}(k\,|\mathbf{x}_{p2}-\mathbf{x}_{pN}|) \\ \vdots & \vdots & & \vdots \\ \operatorname{sinc}(k\,|\mathbf{x}_{pN}-\mathbf{x}_{p1}|) & \operatorname{sinc}(k\,|\mathbf{x}_{pN}-\mathbf{x}_{p2}|) & \cdots & 1 \end{bmatrix} \tag{3.40}$$

where

$$z_o = \frac{\omega^2\,\rho}{4\pi\,c} \tag{3.41}$$

$$Re\{\mathbf{Z}_p(\mathbf{x}_s)\} = Re\{\mathbf{Z}_s(\mathbf{x}_p)^{\mathrm{T}}\} \tag{3.42}$$

Inserting these relationships into Eq (3.37) the total power will be witten as Eq (3.43).

$$\begin{aligned} W_{total} &= \frac{1}{2}\,Re\{\mathbf{q}_s^{\mathrm{H}}\mathbf{Z}_s^{\mathrm{H}}(\mathbf{x}_s)\mathbf{q}_s + \mathbf{q}_p^{\mathrm{H}}\mathbf{Z}_p^{\mathrm{H}}(\mathbf{x}_s)\mathbf{q}_s + \mathbf{q}_s^{\mathrm{H}}\mathbf{Z}_s^{\mathrm{H}}(\mathbf{x}_p)\mathbf{q}_p + \mathbf{q}_p^{\mathrm{H}}\mathbf{Z}_p^{\mathrm{H}}(\mathbf{x}_p)\mathbf{q}_p\} = \\ &= \frac{1}{2}\,[\mathbf{q}_s^{\mathrm{H}}Re\{\mathbf{Z}_s^{\mathrm{H}}(\mathbf{x}_s)\}\mathbf{q}_s + \mathbf{q}_p^{\mathrm{H}}Re\{\mathbf{Z}_p^{\mathrm{H}}(\mathbf{x}_s)\}\mathbf{q}_s + \mathbf{q}_s^{\mathrm{H}}Re\{\mathbf{Z}_s^{\mathrm{H}}(\mathbf{x}_p)\}\mathbf{q}_p + \\ &\qquad + \mathbf{q}_p^{\mathrm{H}}Re\{\mathbf{Z}_p^{\mathrm{H}}(\mathbf{x}_p)\}\mathbf{q}_p] \end{aligned} \tag{3.43}$$

Eq 3.43 can then be written on the form

$$W = \mathbf{q}_s^{\mathrm{H}}\mathbf{A}\mathbf{q}_s + \mathbf{q}_s^{\mathrm{H}}\mathbf{b} + \mathbf{b}^{\mathrm{H}}\mathbf{q}_s + c \tag{3.44}$$

where

$$\mathbf{A} = \frac{1}{2}Re\{\mathbf{Z}_s(\mathbf{x}_s)\} \tag{3.45}$$

$$\mathbf{b} = \frac{1}{2}Re\{\mathbf{Z}_p(\mathbf{x}_s)\}\mathbf{q}_p \tag{3.46}$$

$$c = \frac{1}{2}\mathbf{q}_p^{\mathrm{H}}Re\{\mathbf{Z}_p(\mathbf{x}_p)\}\mathbf{q}_p \tag{3.47}$$

This formulation of the total power is on quadratic form, which results in a minimum of the total power with respect to $\mathbf{q}_s$. The minum for this function is

$$W_{min} = c - \mathbf{b}^{\mathrm{H}}\mathbf{A}^{-1}\mathbf{b} \tag{3.48}$$

$$\mathbf{q}_{s\,min} = -\mathbf{A}^{-1}\mathbf{b} \tag{3.49}$$

For more information of this see (P. A. Nelson 1987) page 407-408.

With this formulation of the minimization of total power, the equation was implemented in a MATLAB program. In this program the number of primary sources, secondary sources and geometry could be changed. The first setup was with one point source as primary source that was controlled by one to four secondary sources. Then the primary source was increased with 60 point sources on row with a length of 0.7 wavelengths. The secondary sources in this case was changed between one to ten sources. The placement for those secondary sources was tested in two different cases, in row and two and two (see Figures 3.5 and 3.7).
The results from this program can be seen in Figures 3.3 - 3.8. In all figures it can be seen that there will be better reduction by placing the secondary sources as close as it can be to the slit. It can also be seen that the more secondary sources that is used the better reduction will be achieved. But with this setup a reduction of 25dB can be achieved with only two secondary sources when they are in row (see Figure 3.6), and that is a high reduction of the radiated noise. So from this results it is enough to use two secondary sources placed on a row, and this will be used for the real experiment. (P. A. Nelson 1987)

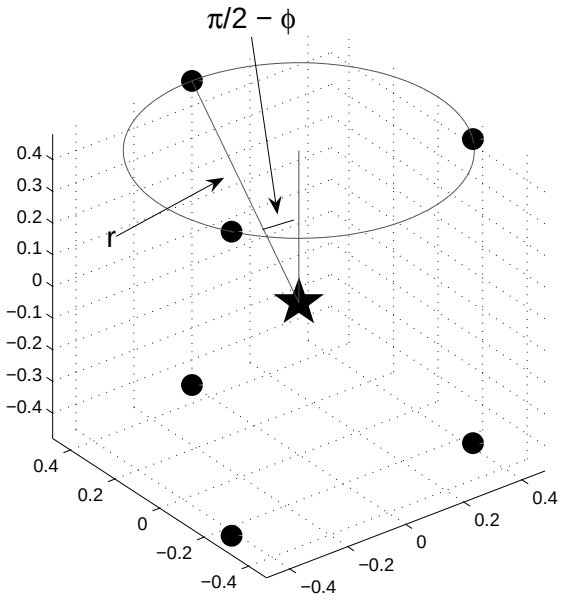

Figure 3.3. Geometrical setup with 1point sorce as primary and several secondary sources

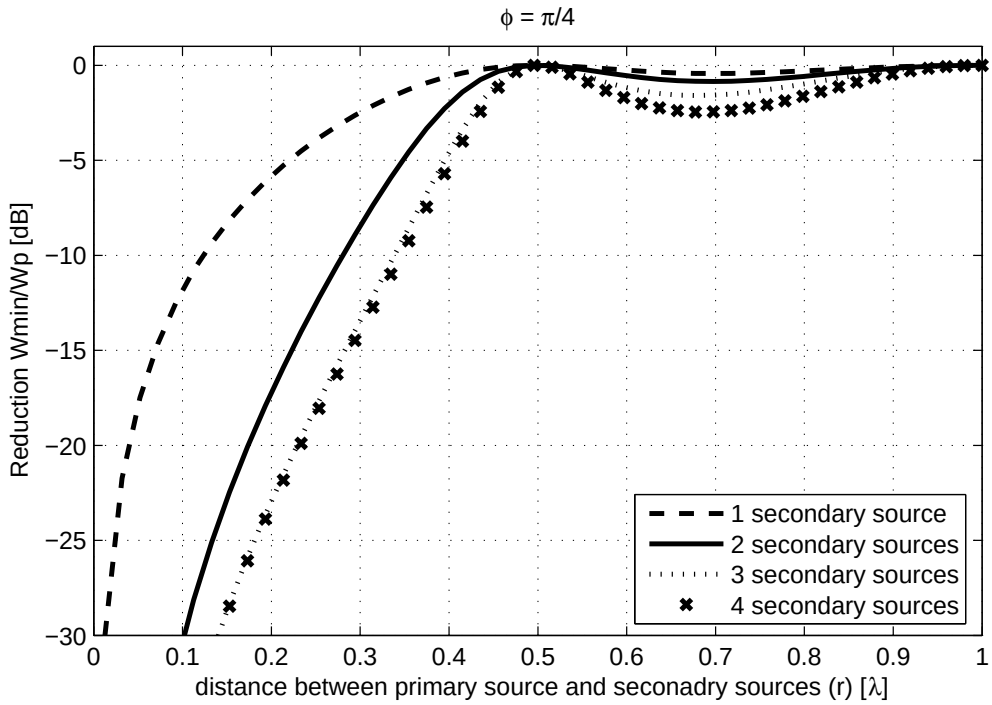

Figure 3.4. 1 point sorce as primary and several secondary sources

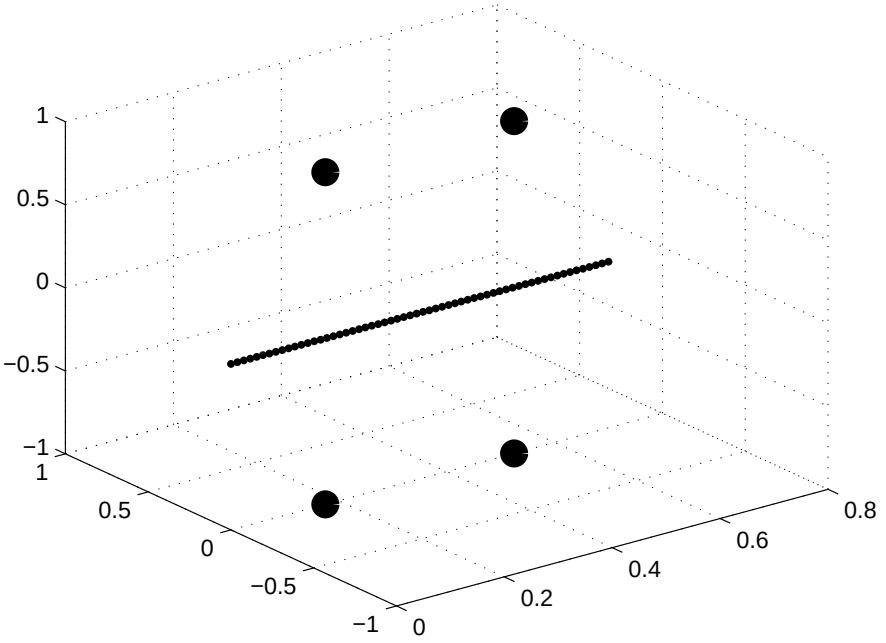

Figure 3.5. Geometrcal setup 60 point sorces as primary and several secondary sources in row.

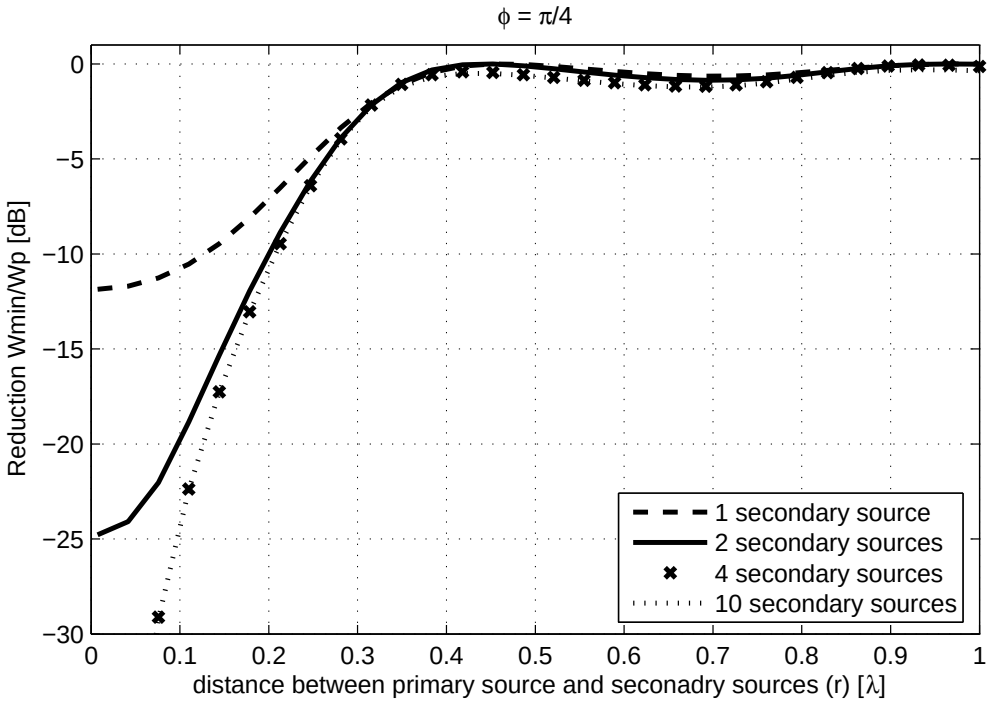

Figure 3.6. 60 point sorces as primary and several secondary sources in row.

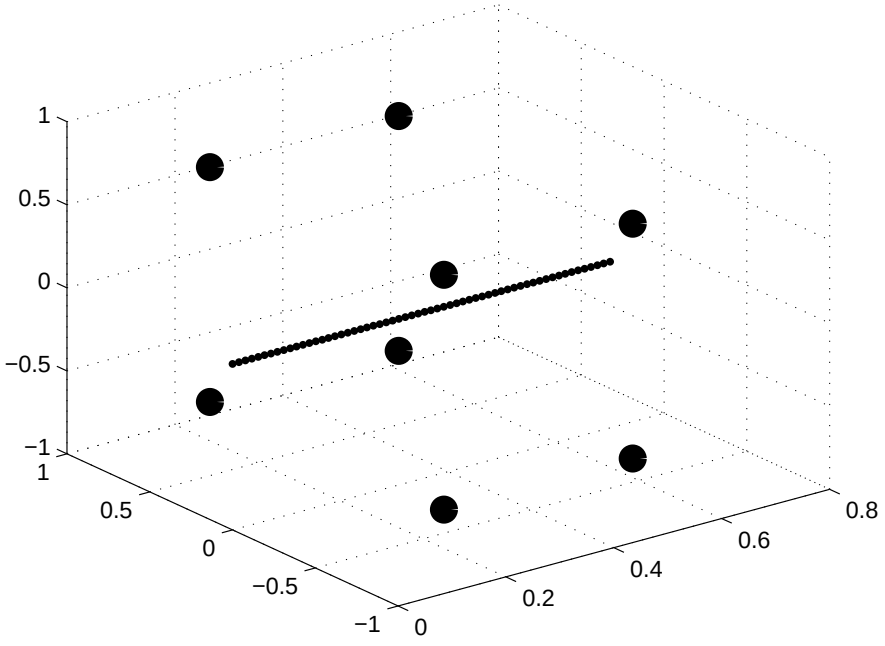

Figure 3.7. Geometrcal setup 60 point sorces as primary and several secondary sources 2 and 2.

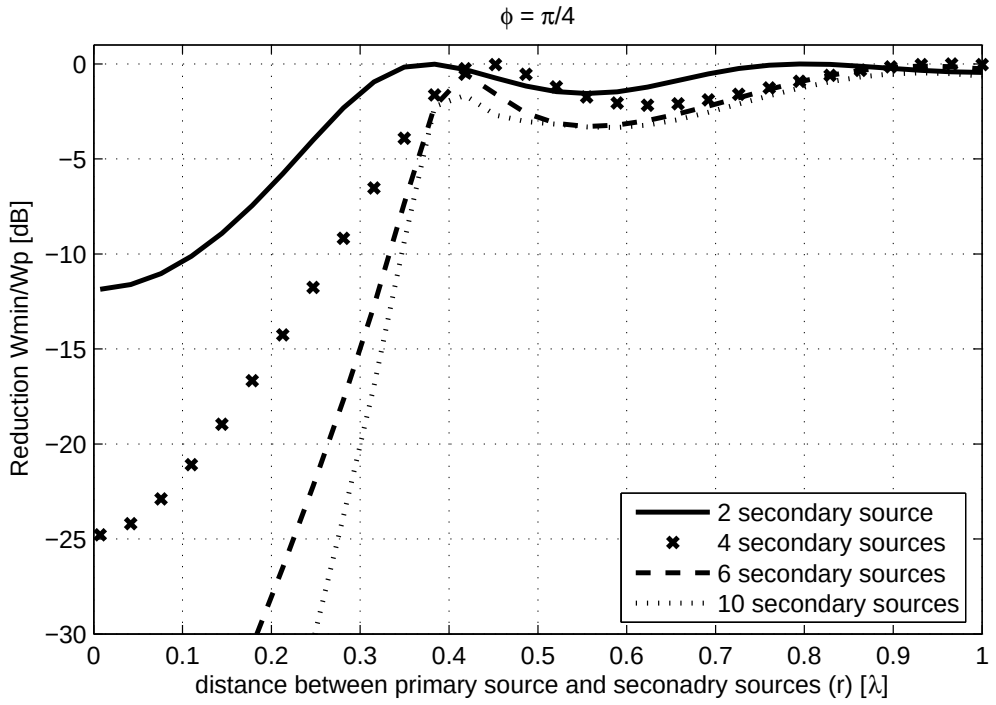

Figure 3.8. 60 point sorces as primary and several secondary sources 2 and 2.

3.2 Measurement of total sound power

In this thesis the goal is to minimize the total radiated sound power from the slit. How can this power be measured? The idea is not to measure exactly the power, but measure something that is proportional to the total power. By minimizing this will result in minimization of the total power.
The total sound power W is defined as:

$$W = S\,I \tag{3.50}$$

$$I = \frac{1}{2}Re(p\,v^*) = \frac{1}{2}Re(\frac{1}{Z}\,|p|^2) \tag{3.51}$$

$S =$ area sourrounding source,
$I =$ sound intensity,
$p =$ sound pressure,
$v =$ particle velocity,

$$Z = \frac{p}{v} \tag{3.52}$$

From Eq 3.50 is the sound power found by measureing the intensity at several positions on a surface that sourrunds the source. The intensity can be found by measureing sound pressure and particle velocity in each point. This can be quite hard, because to measure the particle velocity you need 2 microphones. So the idea is like this.
Measure the sound pressure in several positions on a sphere at some distance away from the source. If the source is in free field and the microphones is placed in the far field of the sound, the intensity will then be proportional to sound pressure squared (the impedance Z in this case is real). Therefore by minimizing the sound pressure squared the sound intensity will also be minimized. By then minimizing the intensity at several positions around the source will result in minimization of the sound power.
Where is far field? Far field in free field is when $k\,r >> 1$, where k is the wave number and r is the distance from source. For instance if the microphone is placed 1m away from a source that is radiating with a frequency a 400 Hz, $kr \approx 8$. Thus by placing microphones 1m from source in the experiment a quit god approximation of the total power from source can be measured by measuring sound pressure squared.
If the source not is placed in free field, it may be placed in a room where the sound field can be assumed to be diffuse. Then by minimizing the sound pressure squared at several positions the total energy density of the sound field will be minimized, which is some measure of total power. Therefore can the placement of the microphones in a sphere like in free field also be used in diffuse field.
How can the total power be minimized? The idea of minimizing the total power is to minimize the total sound pressure squared in a mean square sense for all micpositions. To do this the multichanel filtered X-LMS algorithm will be used.

3.3 The control system

The goal with this thesis is to reduce the total radiated sound power from the slit by adding some secondary sources. But how shall the signals that is fed to the secondary sources be? The goal with this section is to formulate a control algorithm that shall controll the secondary sources so the radiated power is minimized.
As described in section 3.2 the radiated power will be reduced if the sound pressure squared is reduced in several positions around the slit. The complete system can be described in block diagram like Figure 3.9. This is a so called feed forward system with one input signal and several output signals. In Figure 3.9 **x(n)** is the input

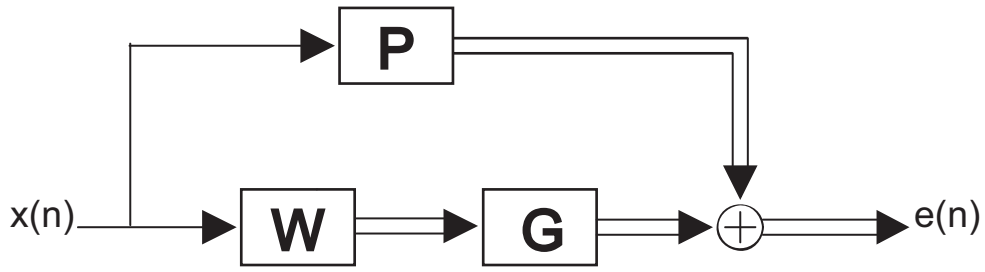

Figure 3.9. Block diagram description of the total system.

signal and **e(n)** is the signals in the microphones which is called error signals (since it is these signals that wants to be minimized). **P** is the transfer functions from the input signal through the slit to the microphones, which is called the primary paths. This block is the model of the real furnace. **G** is transfer functions of our secondary sources, and in this transfer functions it is a lot of parts is included. It is the electronics in the DSP card, the amplifier to secondary sources, the secondary sources, the acoustic path from secondary sources to error microphones and the microphones. This path is called the plant path. **W** is the controll filter, it is the filter coefficients of these filters that will be changed so the total power will be minimized. The thick lines in Figure 3.9 describe that there is several signals and the thin lines is just for one signal. So in our system there is one input signal both to the slit (**P**) and to the filter (**W**). From the slit there is coming sound to several microphones and therefore there is a thick line. The filter sends signals to several secondary sources and from each secondary source a sound field is created that will radiate to all microphones.
The control algorithm that is planned to use for this system is the multichannel XLMS algorithm, since the system has several output signals and several secondary sources. How this algorithm works is described in several steps, since the algorithm is so complex. To start with the LMS algorithm is formulated and it is used to understand the fundamental part of the LMS algorithm (section 3.3.1). After this the LMS algorithm is imported in the same type of system that the furnace has. This algorithm is called the single channel XLMS (section 3.3.2). The last part to get the multichannel XLMS is when the single channel XLMS is imported in a system that has several signals, and this is described in section 3.3.3. From this XLMS algorithm a MATALB program is written. This program is planned to be

used for the real experiment. The validation of this program is in section 3.3.4.

3.3.1 Single channel LMS

The goal with the LMS algorithm is to find the optimal filter that minimize the mean square error (this optimal filter is called the Wiener filter). The LMS algorithm is an iterative method, this mean that the filter coefficients will be changed adaptly. This is done by using the steepest decent algorithm and can be done since the error surface for such a filter has a quadratic shape.
To start with you may assume that there is an electrical disturbance $d(n)$ that shall be minimized. To minimize the disturbance a FIR filter is implemented. This filter

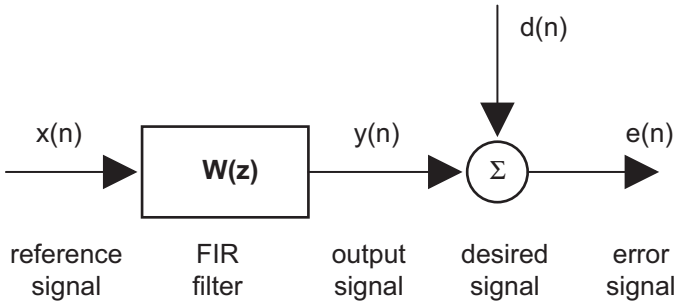

Figure 3.10. Block diagram for the electrical disturbance system.

is fed with a reference signal called $x(n)$ and the output from the filter is called $y(n)$. The error signal is the difference between the desired signal and the output signal from the filter. The output from the filter can be described by the reference signal and the filter coefficients (w_i) for the filter. The error can then be described like this:

$$e(n) = d(n) - \sum_{i=0}^{I-1} w_i \, x(n-i) \tag{3.53}$$

Insted of using a summation over $w_i \, x(n-i)$ as in equation 3.53, the error can be formulated in vectors. Then the the sumation will then be a vector inner product.

$$e(n) = d(n) - \mathbf{w}^{\mathrm{T}}\mathbf{x}(n) = d(n) - \mathbf{x}^{\mathrm{T}}(n)\mathbf{w} \tag{3.54}$$

where

$$\mathbf{w} = [w_0 \; w_1 \; ... \; w_{I-1}]^{\mathrm{T}} \tag{3.55}$$

$$\mathbf{x}(n) = [x(n) \; x(n-1) \; ... \; x(n-I+1)]^{\mathrm{T}} \tag{3.56}$$

Next step is then to find the values of the filter coefficients $w_0 \; ... \; w_{I-1}$ that minimize the quadratic cost function J given by the mean square error.

$$J = E[e^2(n)] \tag{3.57}$$

Using Equation 3.54 the cost function can be written as

$$J = \mathbf{w}^T\mathbf{A}\mathbf{w} - 2\mathbf{w}^T\mathbf{b} + c \tag{3.58}$$

where

$$\mathbf{A} = E[\mathbf{x}(n)\mathbf{x}^T(n)] \tag{3.59}$$
$$\mathbf{b} = E[\mathbf{x}(n)d(n)] \tag{3.60}$$
$$c = E[d^2(n)] \tag{3.61}$$

Here you can see that the cost function (Eq 3.58) i described in a general quadratic form, which tell us that there is a minimum to this function. To minimize this cost function the LMS algorithm will start somewhere on the quadratic shape (set the filter coefficients to some start values e.g zeros) and every time step the filter coefficients will be adjusted a small amount depending on what the local gradient is. Therefore the important thing is to find the local gradient and then change the filter coefficients so the cost function will step in the opposite direction, then the coefficients is bound to move toward the global minimum of the error surface. This method is called the steepest descent algorithm. This adaption algorithm can be written as

$$\mathbf{w}(new) = \mathbf{w}(old) - \mu\frac{\partial J}{\partial \mathbf{w}}(old) \tag{3.62}$$

where μ is a constant that decide how long each step shall be, this is called the convergence factor. In the LMS algorithm an approximation of the gradient is used, which is called the stochastic gradient (Eq 3.63).

$$\frac{\partial e^2(n)}{\partial \mathbf{w}} = -2\mathbf{x}(n)e(n) \tag{3.63}$$

Inserting this approximation of the gradient the LMS algorithm is found (Eq 3.64)

$$\mathbf{w}(n+1) = \mathbf{w}(n) + \alpha\mathbf{x}(n)e(n) \tag{3.64}$$

where $\alpha = 2\mu$ is the convergence coefficient. This can be represented in a block diagram like Figure 3.11.
(Elliott 2001)

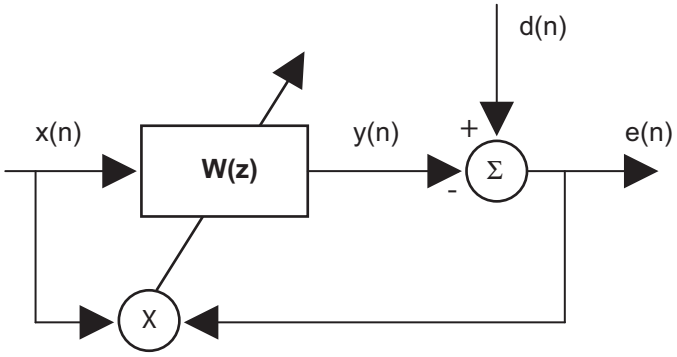

Figure 3.11. Block diagram for the single chanel LMS algorithm

3.3.2 Single chanel XLMS algortithm

In the single channel LMS section the goal was to minimize some electrical noise where the system looked like Figure 3.10. Now if this noise is from an induction furnace and the goal is to minimize the sound pressure in a point. To minimize this noise a speaker is placed and the sound pressure at this point is the sum of the disturbance sound and the sound from the speaker. The signal that is fed to the speaker is found from the magnetic field from the furnace. This type of system is called a single channel feed forward system. The system can be described in block diagram like Figure 3.12a. Here you can see that there is one more block after

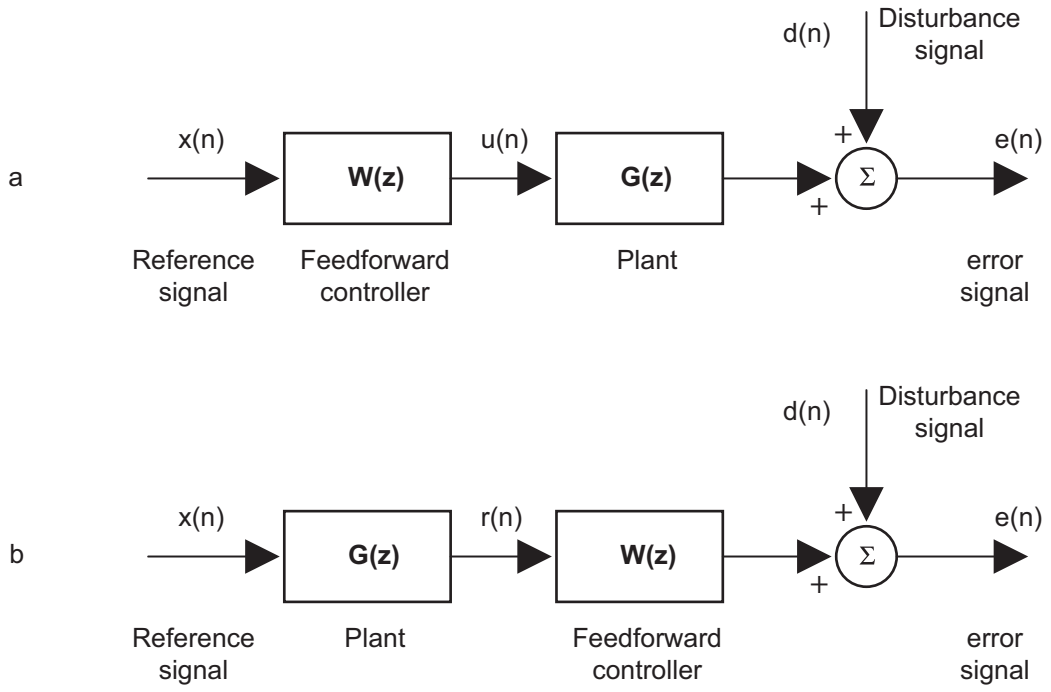

Figure 3.12. Block diagram for the single chanel feedforward system.

the feed forward controller (the filter) which is called the plant path. This block is included since the output signal from the filter is not the sound pressure, it is the

electrical signal that is feed to the amplifier. So before this signal reach the point as a sound pressure it goes through an amplifier , a speaker etc. All these parts has different transfer functions and this plant path is the total transfer function of all these parts. The fact that the systems that we dealing with is linear the blocks can be shifted (Figure 3.12b), then the system look almost the same as in the LMS case. It is now a different input signal to the controller that is called $r(n)$. The error signal then be represented as

$$e(n) = d(n) + \mathbf{w}^T \mathbf{r}(n) \tag{3.65}$$

In this case the LMS algorithm can be written as Equation 3.66 and this is called the filtered-reference LMS or the filtered-x LMS.

$$\mathbf{w}(n+1) = \mathbf{w}(n) - \alpha\, \mathbf{r}(n) e(n) \tag{3.66}$$

In practice, the filtered reference signal will be generated using an estimated version of the true plant response respresented as a plant model called $\hat{G}(z)$. The practical version of the XLMS algorithm can thus be written as

$$\mathbf{w}(n+1) = \mathbf{w}(n) - \alpha\, \hat{\mathbf{r}}(n) e(n) \tag{3.67}$$

This can be represented in block diagram like Figure 3.13
(Elliott 2001)

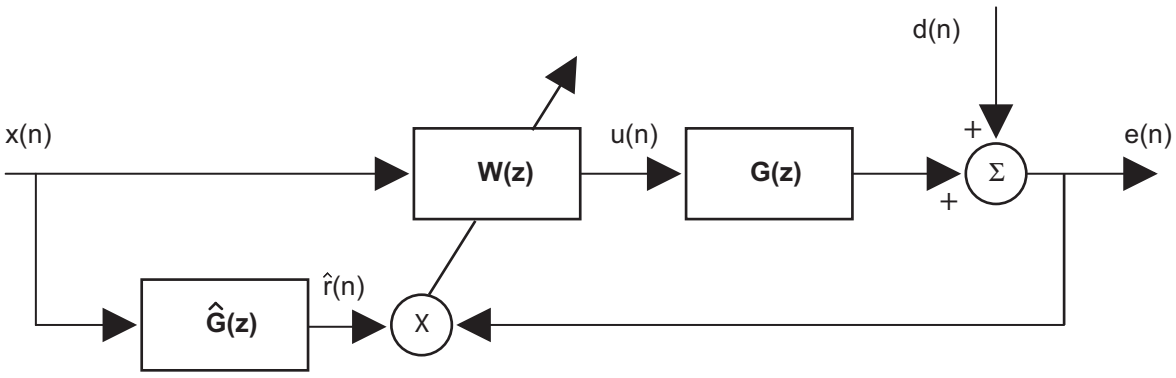

Figure 3.13. Block diagram for the single chanel XLMS algorithm.

3.3.3 Multichanel XLMS

In this part I assume that there is a system that is similar to the system in single channel XLMS algorithm (Figure 3.12). The difference now is that there is K reference signals, M controll inputs, L disturbances and error signals. This can be seen in Figure 3.14. Assume that the FIR control filters each have I coefficients. There are then a total of MKI coefficients to be adapted with the goal to minimize the the sum of squared outputs from all L sensors.

A matrix formulation for the error vector will now be presented. The general l-th

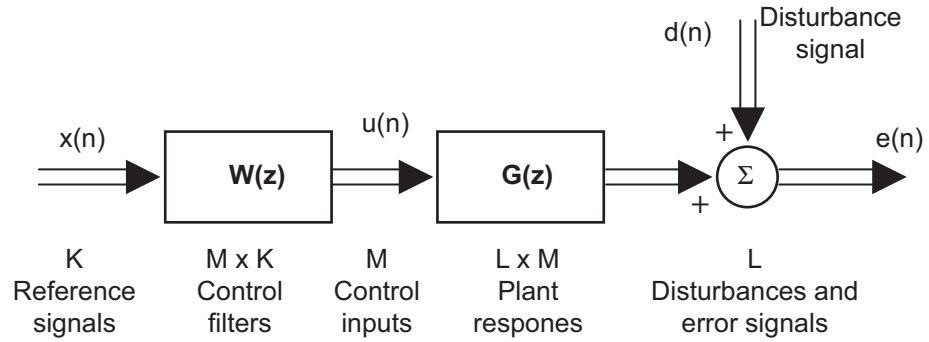

Figure 3.14. Blockdiagram of a general multichanel feedforward control system.

error signal, $e_l(n)$, can be written as the sum of the l-th disturbance, $d_l(n)$, and the contributions from all M secondary actuator signals, $u_1(n)$, ..., $u_M(n)$, filtered by the corresponding elements of the response of the plant, i.e.

$$e_l(n) = d_l(n) + \sum_{m=1}^{M} \sum_{j=0}^{J-1} g_{lmj}\, u_m(n-j) \tag{3.68}$$

where the impuls response of the plant from the m-th to the l-th sensor is represented by the J-th order FIR filter with coefficients g_{lmj}. The signal driving the m-th actuator, $u_m(n)$, is made up of the sum of contributions from K reference signals, $x_1(n)$, ..., $x_K(n)$, each filtered by an I-th order FIR control filter with coefficients w_{mki}, so that

$$u_m(n) = \sum_{k=1}^{K} \sum_{i=0}^{I-1} w_{mki}\, x_k(n-i) \tag{3.69}$$

Inserting Eq 3.68 into Eq 3.69 will give the outputut of the l-th sensor

$$e_l(n) = d_l(n) + \sum_{m=1}^{M} \sum_{j=0}^{J-1} \sum_{k=1}^{K} \sum_{i=0}^{I-1} g_{lmj}\, w_{wki}\, x_k(n-i-j) \tag{3.70}$$

A matrix formulation for the error signal can be obtained by reordering the sequence of filtering for the reference signals, assuming that these filters are time-invariant,

so that Eq 3.70 can be written as

$$e_l(n) = d_l(n) + \sum_{m=1}^{M} \sum_{k=1}^{K} \sum_{i=0}^{I-1} w_{wki}\, \mathbf{r}_{lmk}(n-i) \tag{3.71}$$

where the LMK filtered-reference signals are given by

$$\mathbf{r}_{lmk}(n) = \sum_{j=0}^{J-1} g_{lmj}\, x_k(n-j) \tag{3.72}$$

The inner product in Eq 3.71 can be represented in vector form as

$$e_l(n) = d_l(n) + \sum_{i=0}^{I-1} \mathbf{w}_i^{\mathrm{H}}\, \mathbf{r}_l(n-i) \tag{3.73}$$

where

$$\mathbf{w}_i = [w_{11i}\ w_{12i}\ \ldots\ w_{1Ki}\ w_{21i}\ \ldots\ w_{MKi}]^{\mathrm{T}} \tag{3.74}$$

and

$$\mathbf{r}_l(n) = [r_{l11}(n)\ r_{l12}(n)\ \ldots\ r_{l1K}(n)\ r_{l21}(n)\ \ldots\ r_{lMK}(n)]^{\mathrm{T}} \tag{3.75}$$

The vector of all L error signals,

$$\mathbf{e}(n) = [e_1(n)\ \ldots\ e_L(n)]^{\mathrm{T}} \tag{3.76}$$

can now be written in terms of the vector of disturbances

$$\mathbf{d}(n) = [d_1(n)\ \ldots\ d_L(n)]^{\mathrm{T}} \tag{3.77}$$

and the contribution s from all the secondary sources as

$$\mathbf{e}(n) = \mathbf{d}(n) + \mathbf{R}(n)\, \mathbf{w} \tag{3.78}$$

where

$$\begin{bmatrix} \mathbf{r}_1^{\mathrm{T}}(n) & \mathbf{r}_1^{\mathrm{T}}(n-1) & \ldots & \mathbf{r}_1^{\mathrm{T}}(n-I+1) \\ \mathbf{r}_2^{\mathrm{T}}(n) & \mathbf{r}_2^{\mathrm{T}}(n-1) & \ldots & \mathbf{r}_2^{\mathrm{T}}(n-I+1) \\ \vdots & \vdots & & \vdots \\ \mathbf{r}_L^{\mathrm{T}}(n) & \mathbf{r}_L^{\mathrm{T}}(n-1) & \ldots & \mathbf{r}_L^{\mathrm{T}}(n-I+1) \end{bmatrix} \tag{3.79}$$

and the vector containing all MKI control filter coefficients is defined as

$$\mathbf{w} = [\mathbf{w}_0^{\mathrm{T}}\ \mathbf{w}_1^{\mathrm{T}}\ \ldots\ \mathbf{w}_{I-1}^{\mathrm{T}}]^{\mathrm{T}} \tag{3.80}$$

The vector error signal is now formulated by Eq 3.78 and for the multichanel XLMS algorithm it will adjust each of the control filter coefficients to minimize the instantaneous cost function. The cost function in this case is given by the sum of squared outputs of the error signlas, which can be written as

$$\mathbf{e}^{\mathrm{T}}(n)\mathbf{e}(n) = \mathbf{w}^{\mathrm{T}}(n)\mathbf{R}^{\mathrm{T}}(n)\mathbf{R}(n)\mathbf{w}(n) + 2\mathbf{w}^{\mathrm{T}}(n)\mathbf{R}^{\mathrm{T}}(n)\mathbf{d}(n) + \mathbf{d}^{\mathrm{T}}(n)\mathbf{d}(n) \tag{3.81}$$

The derivatives of this cost function with respect to the vector of filter coefficients at the same sample time can be written as

$$\frac{\partial\, \mathbf{e}^{\mathrm{T}}(n)\mathbf{e}(n)}{\partial\, \mathbf{e}(n)} = 2\,[\,\mathbf{R}^{\mathrm{T}}(n)\mathbf{R}(n)\mathbf{w}(n) + \mathbf{R}^{\mathrm{T}}(n)\mathbf{d}(n)\,] \tag{3.82}$$

Using Eq 3.78 this vector of derivatives can also be written as

$$\frac{\partial\, \mathbf{e}^{\mathrm{T}}(n)\mathbf{e}(n)}{\partial\, \mathbf{e}(n)} = 2\,\mathbf{R}^{\mathrm{T}}(n)\mathbf{e}(n) \tag{3.83}$$

This vector of the derivatives of squared error are now used to adapt the control filter coefficients in the multichanel XLMS algorithm, wich will be

$$\mathbf{w}(n+1) = \mathbf{w}(n) - \alpha\,\mathbf{R}^{\mathrm{T}}(n)\mathbf{e}(n) \tag{3.84}$$

where α is a convergence coefficient. In practice, the true matrix of the plant responses is not usual available to generate the filtered reference signals and therefore a model of the plant must be used. This plant model is denoted as $\hat{\mathbf{R}}(n)$, and the practical for of the multichannel XLMS algorithm is thus

$$\mathbf{w}(n+1) = \mathbf{w}(n) - \alpha\,\hat{\mathbf{R}}^{\mathrm{T}}(n)\mathbf{e}(n) \tag{3.85}$$

which can be represented in block diagram like Figure 3.15.

(Elliott 2001)

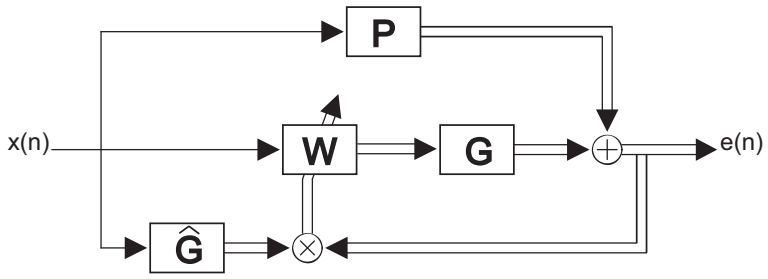

Figure 3.15. Block diagram for the multichannel XLMS algorithm.

3.3.4 XLMS program

To be able to use this XLMS algorithm for the experiment it can either be implemented in real time on a DSP card or implemented on a software program. In this thesis a program that is written in MATALB is used. The goal with the program is to find the filter coefficients that minimize the radiated power. To be able to use the program for the real experiment the transfer functions from the experiment setup must be measured and implemented in the program. But before using this program in the real experiment a validation of it is made. In this validation the input signal will be tonal with a frequency of 400 Hz. The sound pressure will be controlled at 3 error positions, by 1 control source that will be controlled by a FIR filter with 2 coefficients. The primary- and secondary paths is assumed to be Green functions. The block diagram of the validation can be seen in Figure 3.16.

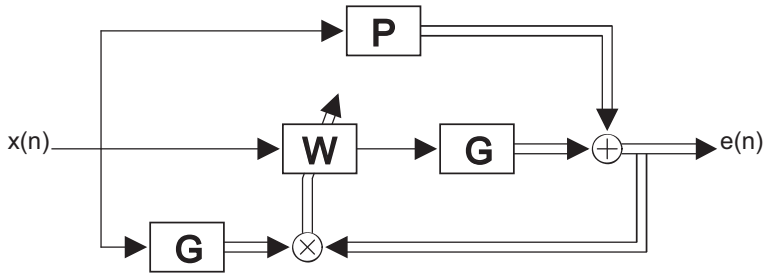

Figure 3.16. Block diagram for the validation of the program.

Running the simulation in 1.2 s will give the result in Figure 3.17. You can see that the algorithm behaves as expected. It converge to stable values for the 2 filter coefficients. The SPL at all 3 microphone positions is reduced more than 30 dB. The summation of pressured squared from all mic positions (our measurement of the total power) is also reduced by around 35 dB.

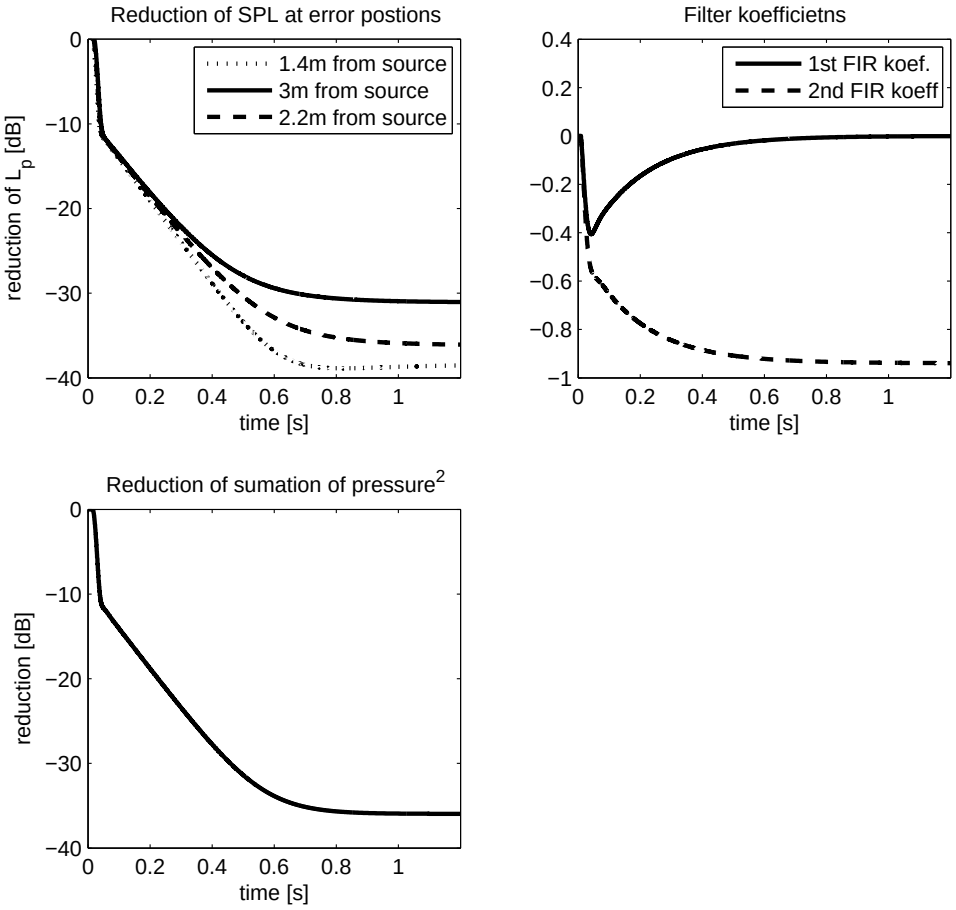

Figure 3.17. Results from the validation of the program.

From this validation the program works as expected and can now be used for the real experiment.

3.4 Conclusion from the theory part

From the simulation in frequency part it can be seen from all pictures that the closer secondary sources is placed the primary source, the better reduction of the total power can be archived. From the frequency part it shows also that there will be better reduction by using several secondary sources. Comparing the two different geometrical setups (Figure 3.6 and Figure 3.8) it can be seen that you will archive better reduction when secondary sources are in row. For instance for two secondary sources the maximum reduction for the setup case two and two (Figure 3.8) is 12dB and for secondary sources with the setup in row (Figure 3.6) it is 25dB.
From this frequency simulation part the conclusion is to place secondary sources in a row and use several secondary sources. For the experiment I will use two secondary sources, because it can give a reduction of 25dB which is a high reduction of the radiated noise.
In the time simulation part it could be seen that the multichannel XLMS was working as expected and to get a better model the transfer functions from the real experiment will be used.

4 EXPERIMENT

The goal with this experiment is to see if the sound field from a slit can be controlled in reality. The sound field from the slit will be created in two ways. In the first case the particle velocity of the slit is in phase for the whole slit. In the second case the first half of the slit is in phase and the second half is out of phase with respect to the first half (these cases can be seen in Figure 2.3). The frequency of the sound from the slit will also be changed, this to exam what happens if the length of the slit, in point of views of wavelengths, i changed.

4.1 Building of acoustic sources

The goal is to build an acoustic source that should generate a sound field from a slit. The particle velocity from this opening shall be changed in different ways. From the frequency simulations it was found that it can be hard too control the sound if the slit is to long. Therefore a slit with a length of 0.6m was built. For a frequency of 400Hz the slit will correspond to a length of about 0,7 wavelengths. If a longer slit is desired the frequency should may be increased e.g. 1kHz will give you a slit that is around 1,8 wavelengths long. Therefore with this physical length of the slit you can get every length in wavelengths you want, just change the frequency.
The sound field from the slit shall be changed in different ways. To be able to do this the source was built like Figure 4.1. In the figure you can see that the speaker

Figure 4.1. Illustration of the slit speaker.

is divided in two sections. This so the particle velocity of the slit can be changed in the two cases "in phase" and "out of phase" mentioned above.
The speaker units that is used in the sections are mounted in a closed box and are ordinary 6.5 inch speaker units. In the sections there are also some absorber mate-

rial placed. This to get less influence of resonances for the speaker. In Figure 4.2 the built speaker can be seen.

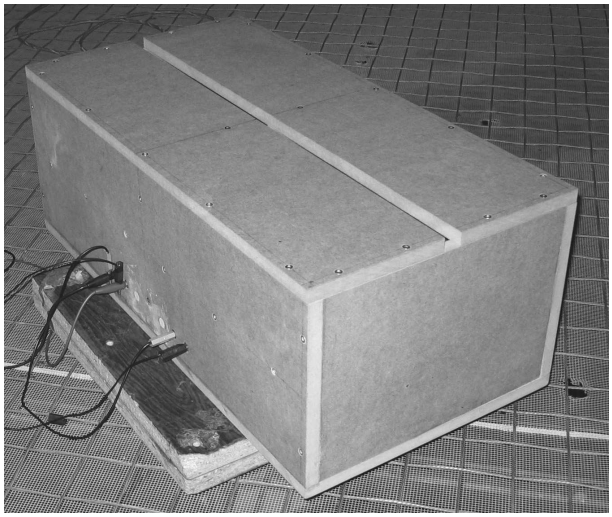

Figure 4.2. Speaker in reality.

To see if the real speaker behaves like expected, the directivity of the speaker was measured. This was then compared with the directivity of slit with the same dimensions calculated theoretically. Due to symmetry the directivity was measured 1.5m away from the slit and for a quarter of a half sphere surrounding the slit, see Figure 4.3.

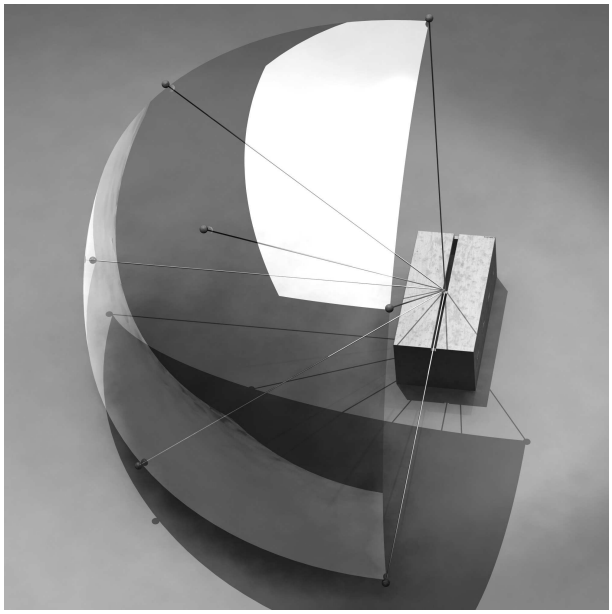

Figure 4.3. Idea of measurement positions of the directivity.

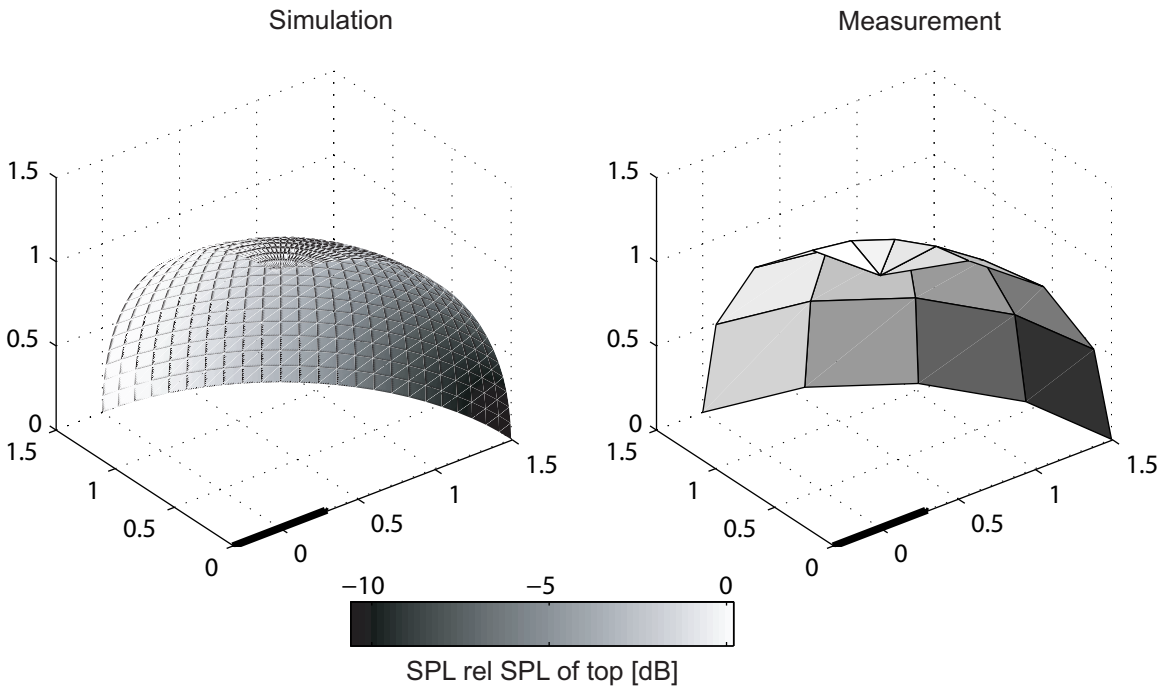

Figure 4.4. Directivity measurement vs. directivity from theory.

From the study of the directivity from the speaker and the theoretical slit (Figure 4.4) it can be seen that the directivity is almost the same for both cases. At the sides of the slit the sound pressure are 10dB lower than above the slit. At the front of the slit the sound pressure is almost the same as above the slit. Therefore it can be assumed that the speaker only radiates from the slit and the speaker behaves as expected.
To build the control sources (also called secondary sources) there is a problem to place the speakers close the opening. For a real induction furnace the slit opening is usually very hot, and that will probably lead to broken speakers. Therefore the idea is to lead the sound from the speakers to the slit like Figure 4.5.

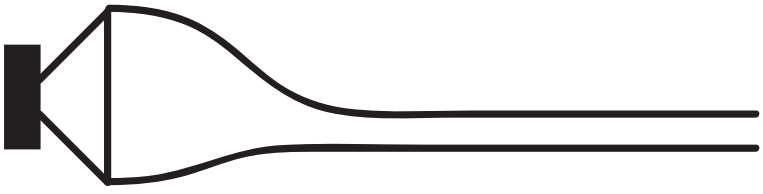

Figure 4.5. Idea for secondary source.

For this experiment the sound from secondary sources is led by plastic tubes. The important with the tubes is that they are rigid, and if these sources is implemented for a real furnace the tubes maybe can consist of some metal or be concrete.
As speakers for the secondary sources 1 inch drivers is used, this since it is easy to lead the sound from this type of speaker to the tube and they where avalible at the department (see Figure 4.6).

A problem with this drivers is that they are designed to generate sounds for mid-

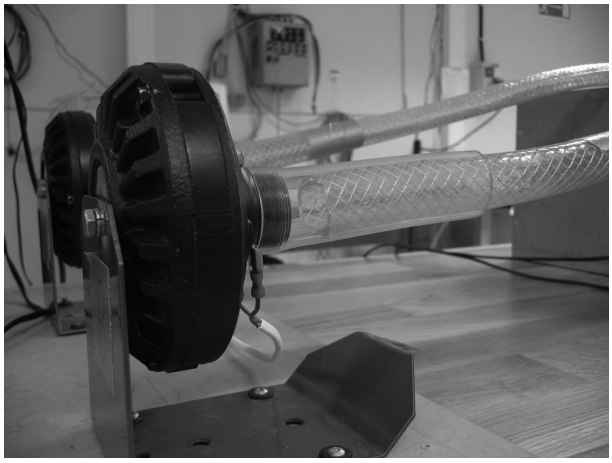

Figure 4.6. Secondary sources in reality.

and high frequencies (1-20kHz). This will result in some distortion for the drivers at lower frequencies. But if it can be shown that the problem is the drivers they can easily be changed in future projects. The caracter of the driver can be seen in Figure 4.7 where a frequency of 400Hz is fed to the secondary system from the VXI-station. The electrical signals before speaker, before amplifier and the sound pressure from secondary source is measured. From this measurement it can be seen that it is the drivers that generate these overtones (the distortion).

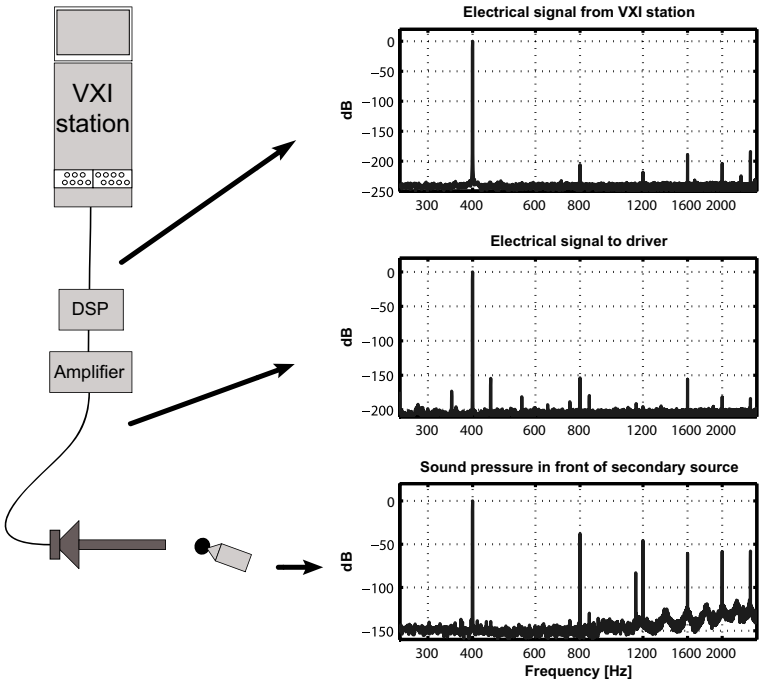

Figure 4.7. Autospectrum of signals around the driver.

In Figure 4.8 can the slit speaker and the two controll sources be seen when they are placed for the experiment.

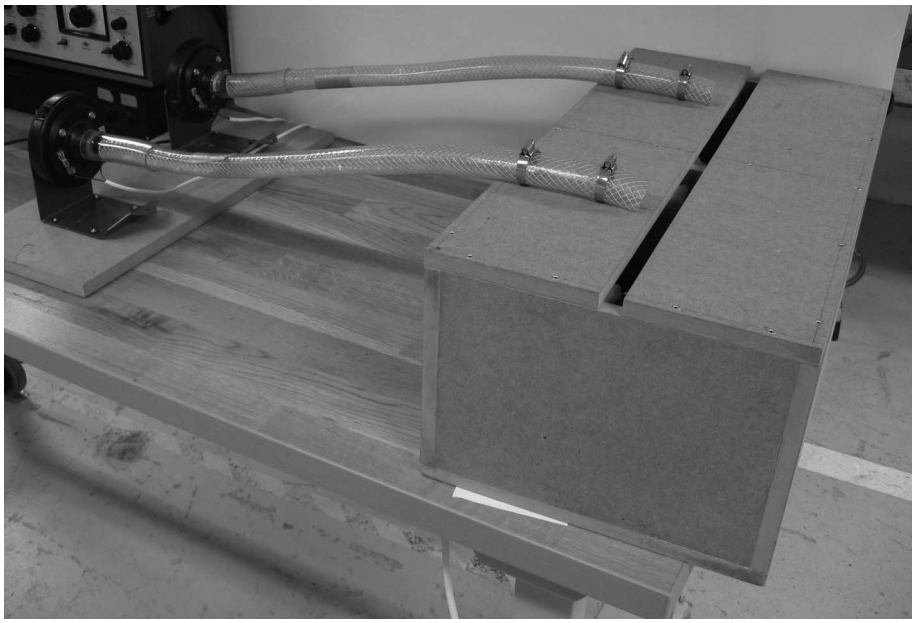

Figure 4.8. Sources in the experiment.

4.2 Equipment

For the experiment this equipent was used:

- Power amplifier, 4ch Yamaha M-35
- VXI measurement station
- microphones, cheap electret
- power supply for the microphones, made at Chalmers
- 2ch DSP card, Analog Devices ADSP-2181
- 2 drivers for the secondary sources, EV 1824S
- plastic tubes for the secondary sources
- special slit speaker
- Sine generator, Bruel and Kjaer type 1027
- 3 sound level meters, TES 1350A

4.3 Setup

The experiment was performed in the vibrolab at Applied Acoustics Chalmers University of technology. The dimensions of the room are 5,5x10,5x2.5m and have concrete floor and walls. In the ceiling there is damping material. The experiment was performed in the middle of the room, and for all measurements the temperature and humidity was around 20^{o}C and 20%.
The idea of measuring the total power was to place nine microphones at 1.1m away from the slit like a part of a sphere (see Figure 4.10 and 5.13).
The importance with this experiment was not to measure the total power exactly, but to compare the result from the measurements with and without active control. The total setup for all components as microphones, speakers, DSP card etc. can be seen in Figure 4.9.

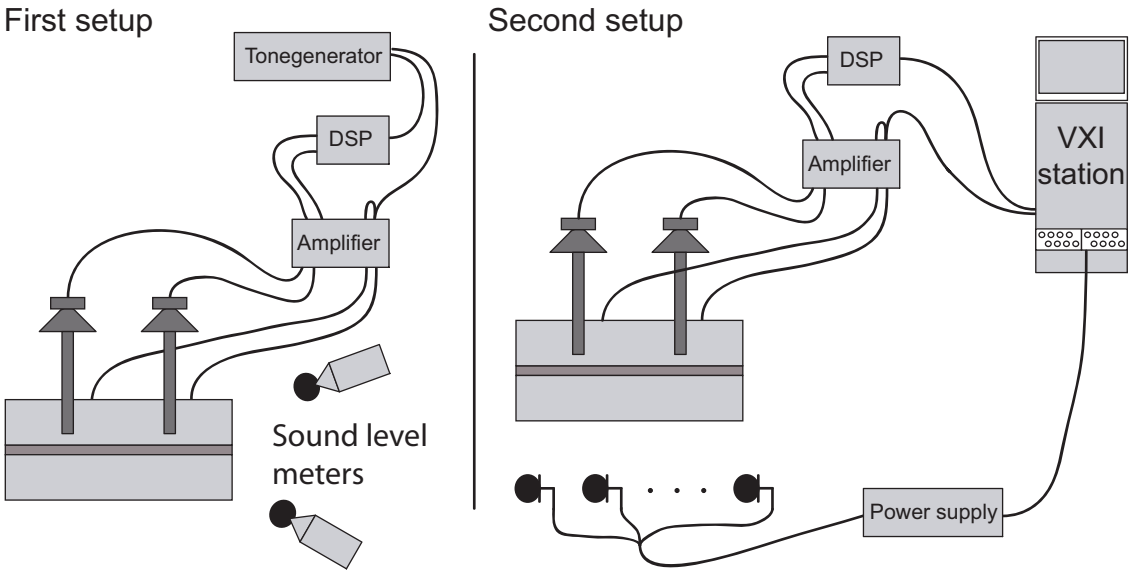

Figure 4.9. Illustration of the setup for the experiment

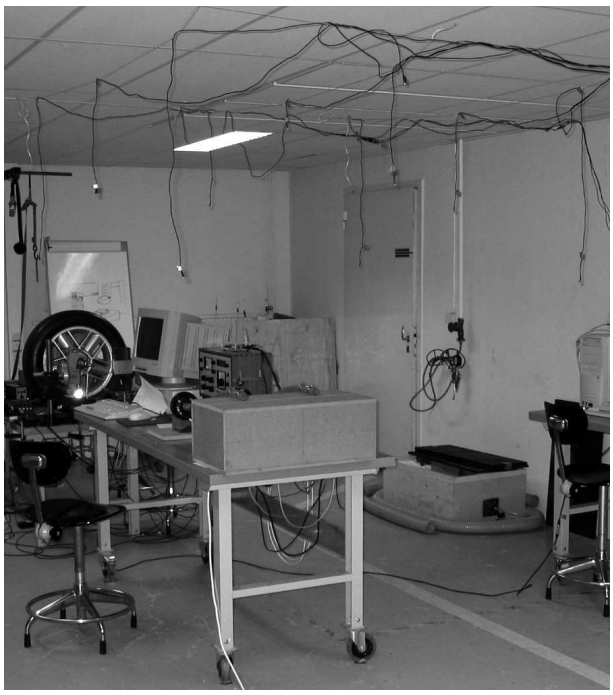

Figure 4.10. Setup for microphones

4.4 Procedure

The first thing to do was to measure all transfer functions (TF's) from the three speakers ,the slit speaker and the two controll speakers, to all nine microphones. This was done by using the second setup in Figure 4.9. In the VXI-station a software called Bullerby was used. In Bullerby white noise was created as input signal to the system and was fed to each speaker one by one. The sampling frequency was 10kHz, block size = 8192 samples. For all measurement the input signal from VXI-station and all nine microphones where measured. Thus to get all transfer functions for the whole system there were four measurements (one measurement for each control speaker and two measurements for the slit speaker for the two different sound fields, "in phase", "out of phase"). In Bullerby software there was some post processing (see Appendix), and out from the software the frequency response functions (FRFs) from source to all microphones was archived.
These FRF's were then implemented on the multichannel XLMS program that was created in the theory part. The goal with this program was to find the filter coefficients for the filter. In this program the frequency that should radiate from the slit must be chosen. For this experiment three different frequencies was examined, 400Hz, 425Hz and 900Hz. These frequencies correspond to a length of the slit of 0.7λ, 0.8λ and 1.6λ (λ = wavelength). For every frequency the two different sound fields from the slit was examined, "in phase", "out of phase". Thus a total of six different setups of the sound from the slit were examined.
When the filter coefficients then where found from the XLMS program these were implemented on the DSP card.

Initially a tonegenerator was used as input signal to see if the system was working. (first setup in Figure 4.9), this so the control system could easily be turned on and off. Then it was easy to hear if it was any difference. There were also used simple sound level meters at different positions, this to get a quick overview over the sound field. To get a more accurate measurement of the control system, the VXI-system was again used with the same microphones that was used for the FRF measurement (second setup in Figure 4.9).

5 RESULTS

5.1 400Hz, particle velocity "in phase"

In Figure 5.1 the time domain simulation can be seen when the particle velocity of the slit is in phase and has a frequency of 400 Hz. The results for the real experiment when the filter coefficients is imported from simulation can be seen in Figure 5.2.

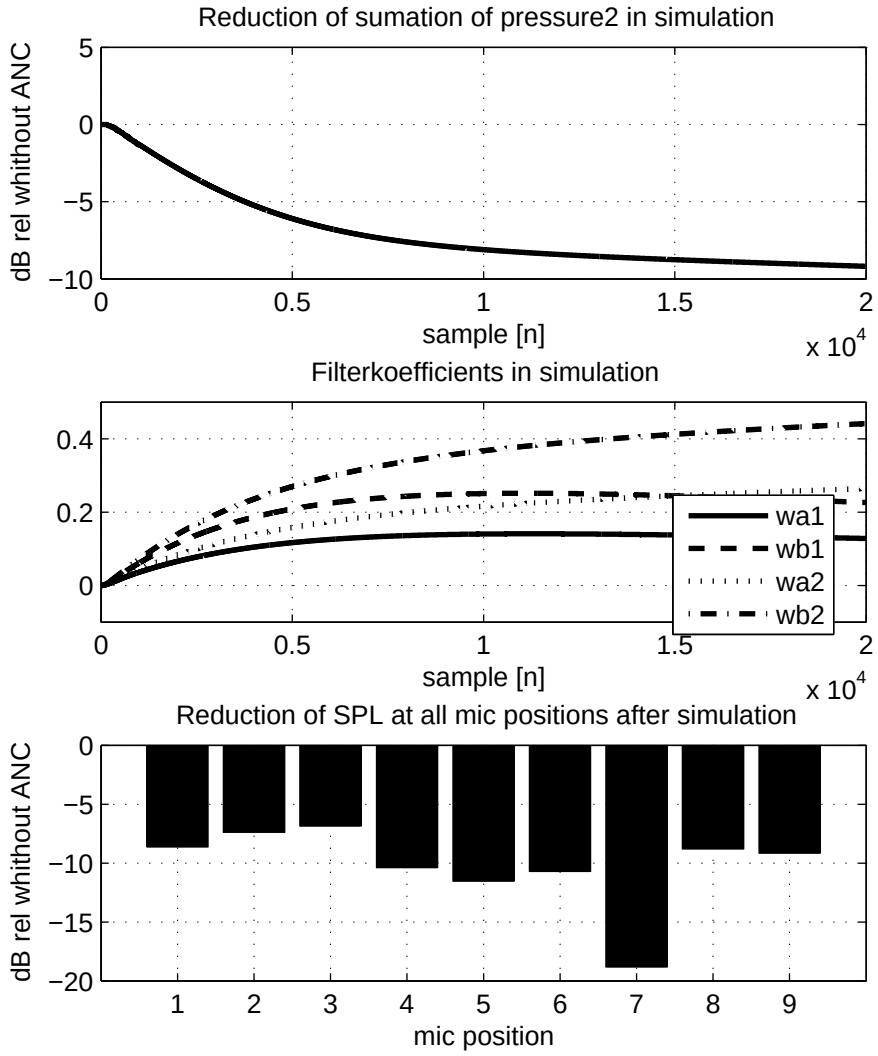

Figure 5.1. Simulation when frequency is 400Hz, particle velocity is "in phase".

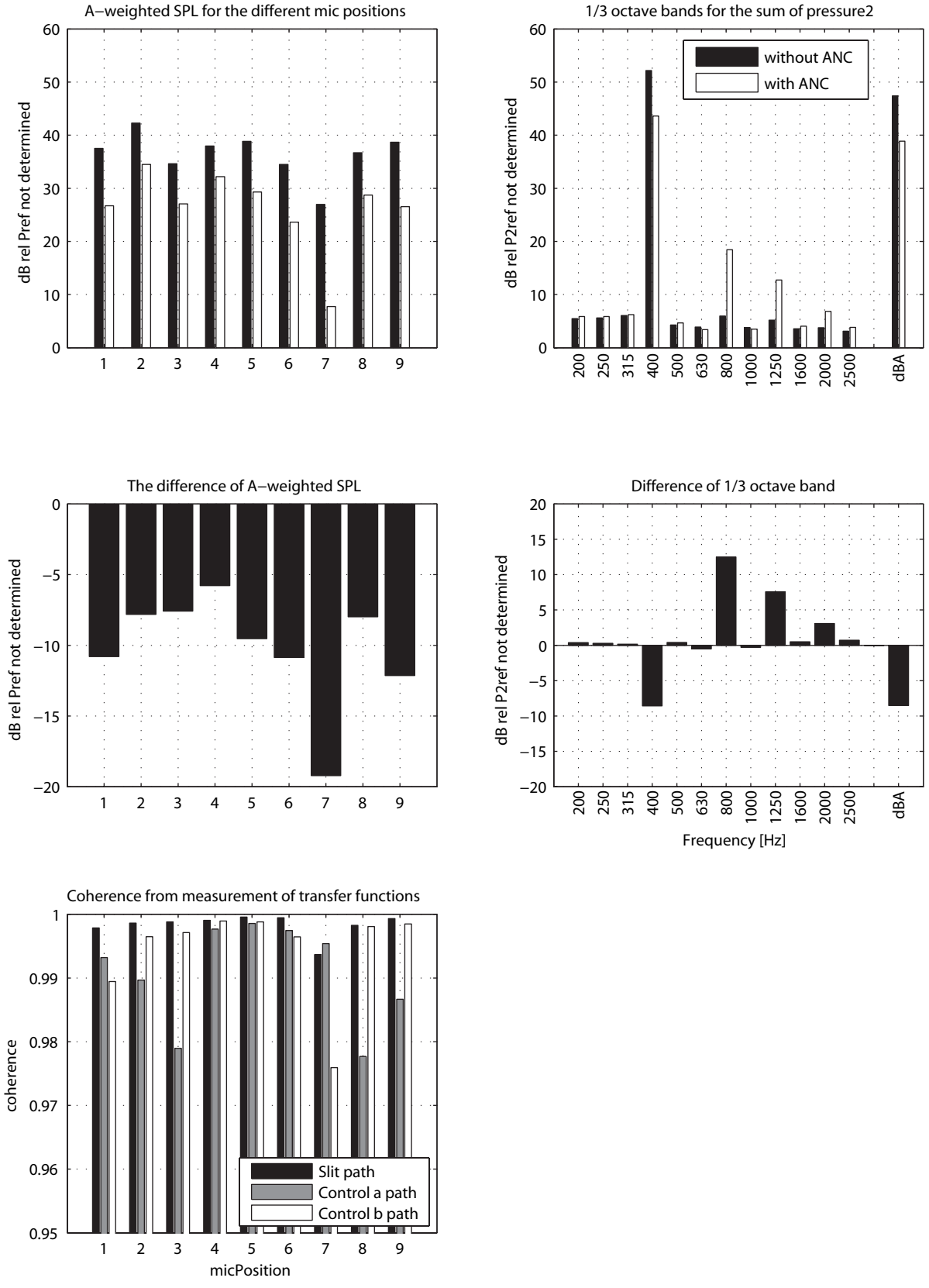

Figure 5.2. Experiment when frequency is 400Hz, particle velocity of slit is "in phase".

5.2 400Hz, particle velocity "out of phase"

In Figure 5.3 the time domain simulation can be seen when the particle velocity of the slit is out of phase and has a frequency of 400 Hz. The results for the real experiment when the filter koefficients is imported from simulation can be seen in Figure 5.4.

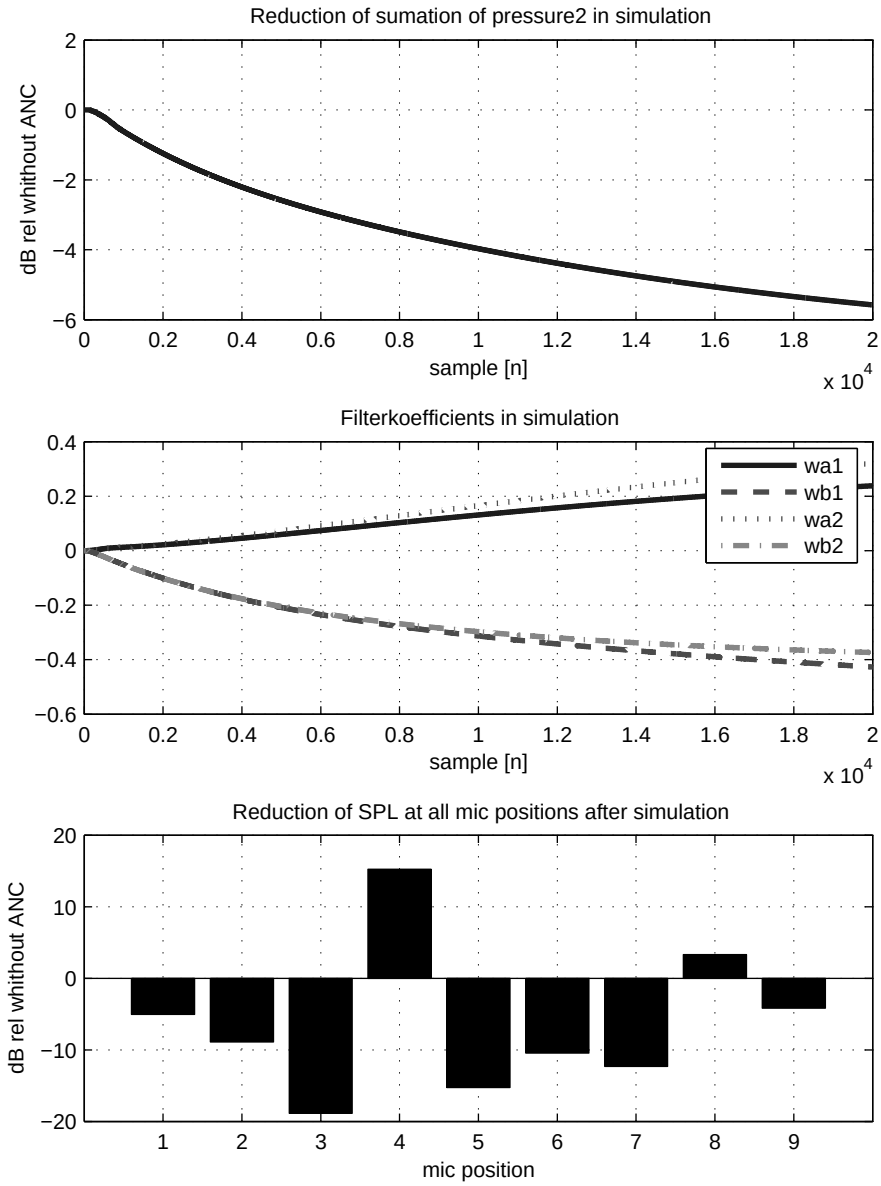

Figure 5.3. Simulation when frequency is 400Hz, particle velocity is "out of phase".

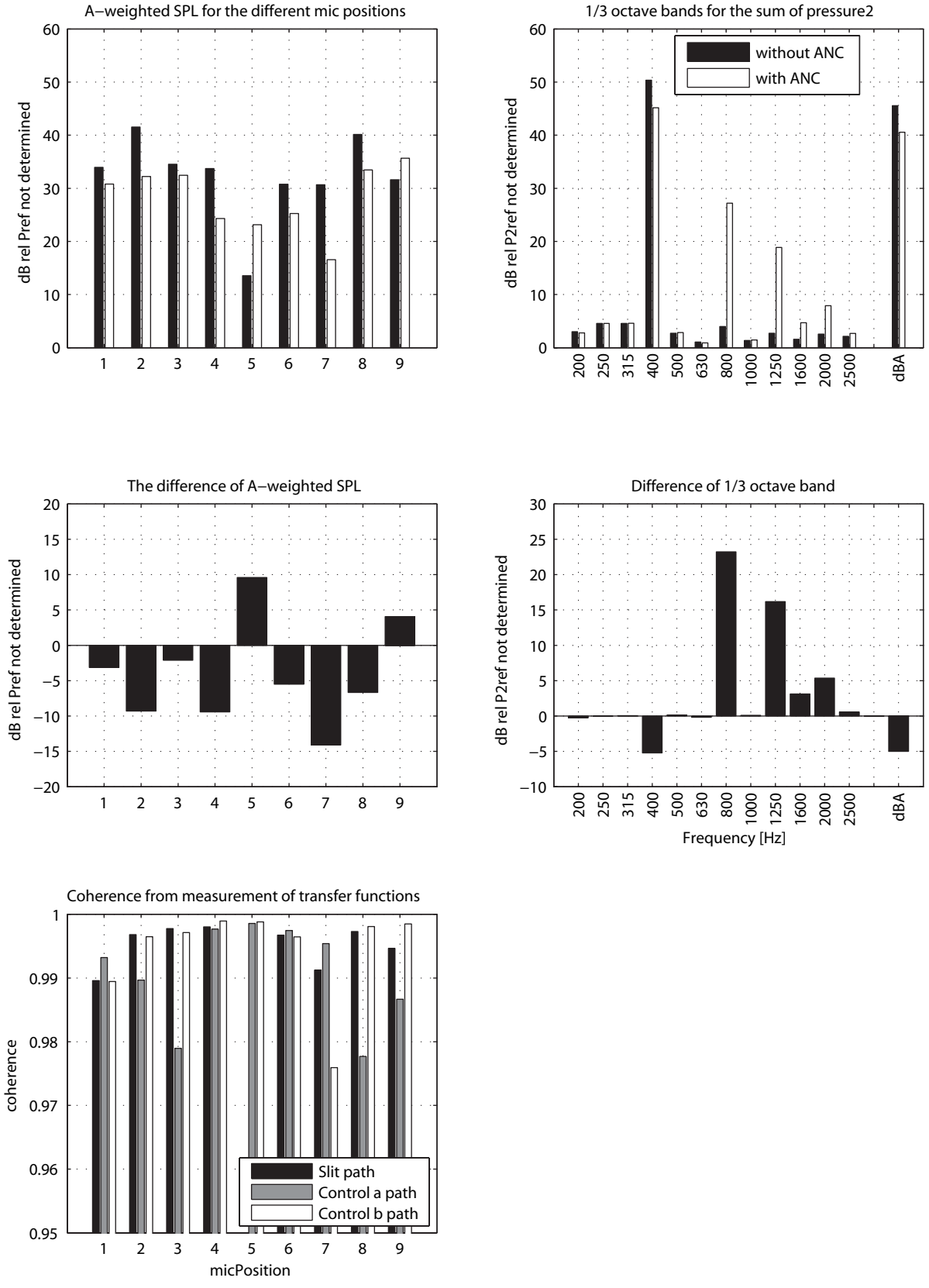

Figure 5.4. Experiment when frequency is 400Hz, particle velocity of slit is "out of phase".

5.3 425Hz, particle velocity "in phase"

In Figure 5.5 the time domain simulation can be seen when the particle velocity of the slit is in phase and has a frequency of 425 Hz. The results for the real experiment when the filter koefficients is imported from simulation can be seen in Figure 5.6.

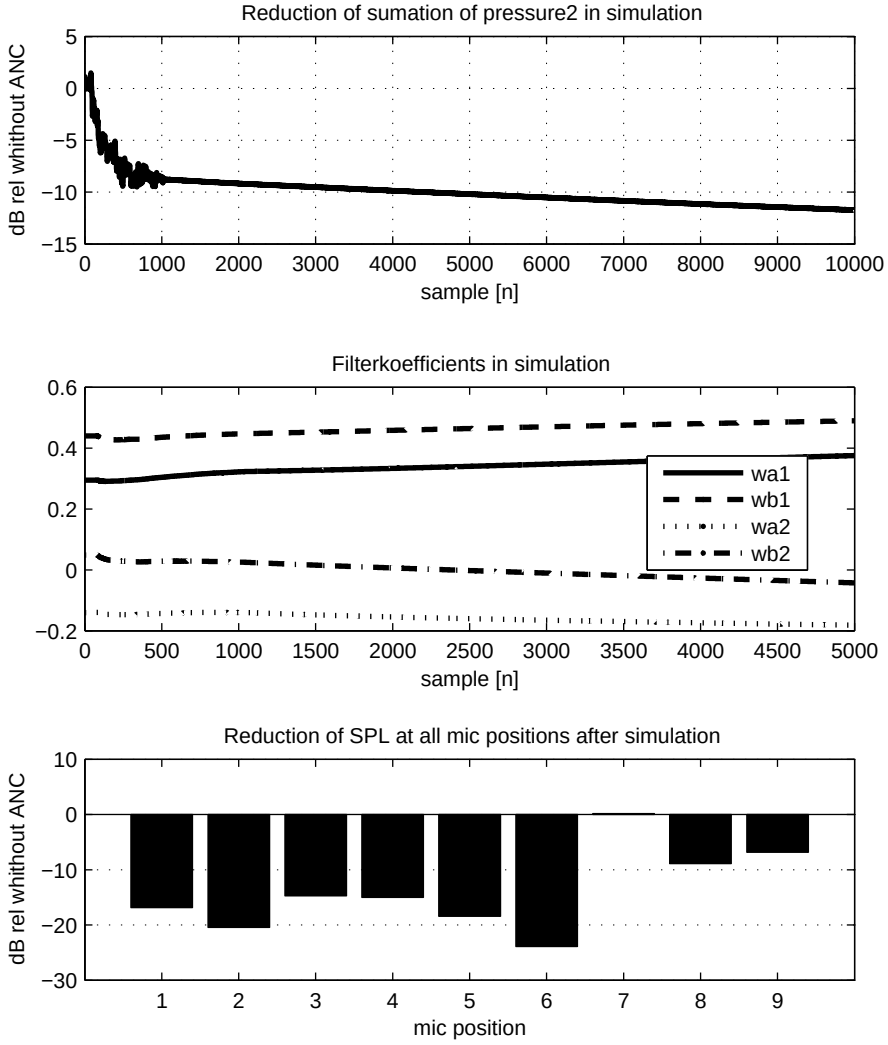

Figure 5.5. Simulation when frequency is 425Hz, particle velocity is "in phase".

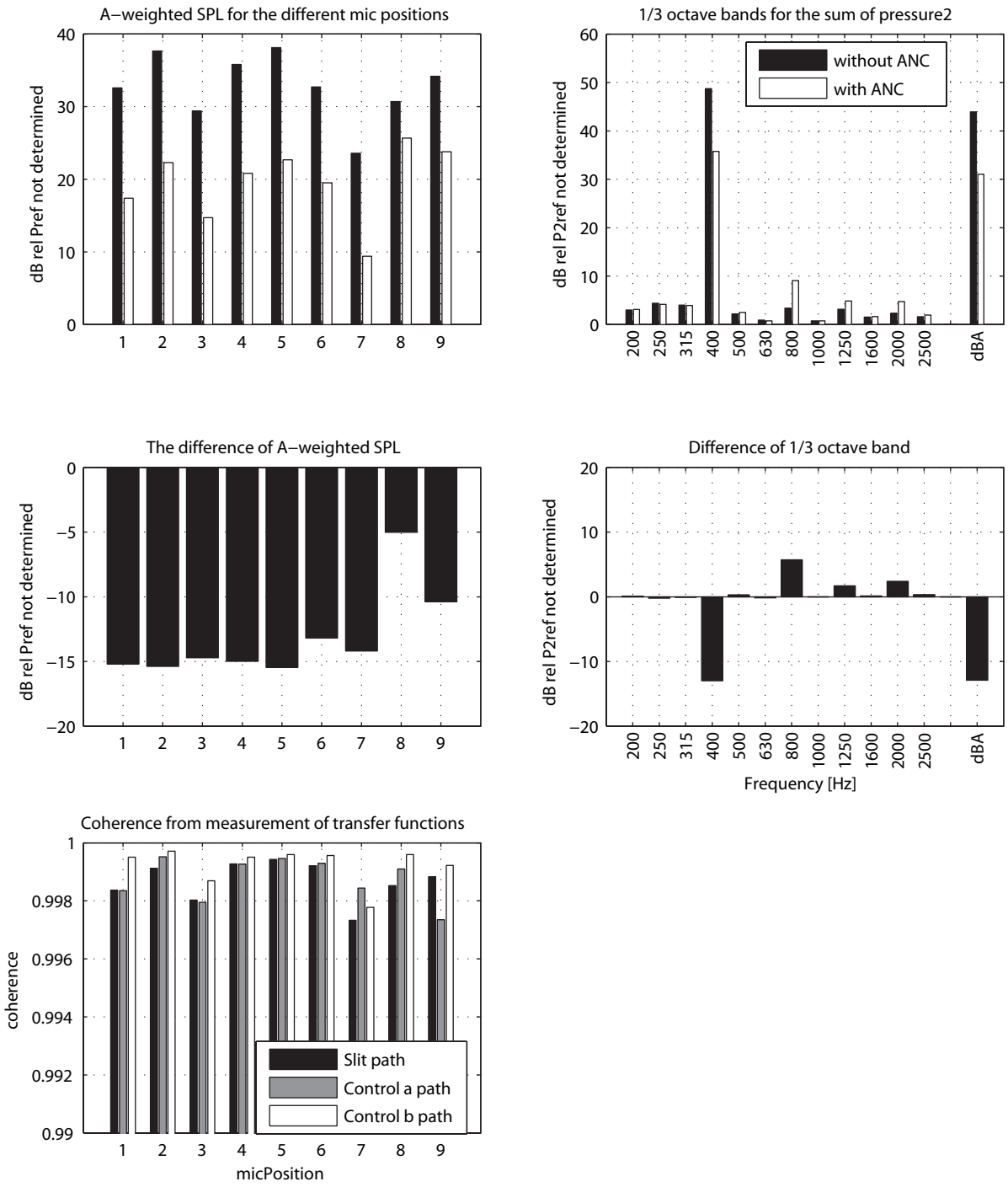

Figure 5.6. Experiment when frequency is 425Hz, particle velocity of slit is "in phase".

5.4 425Hz, particle velocity "out of phase"

In Figure 5.7 the time domain simulation can be seen when the particle velocity of the slit is out of phase and has a frequency of 425 Hz. The results for the real experiment when the filter koefficients is imported from simulation can be seen in Figure 5.8.

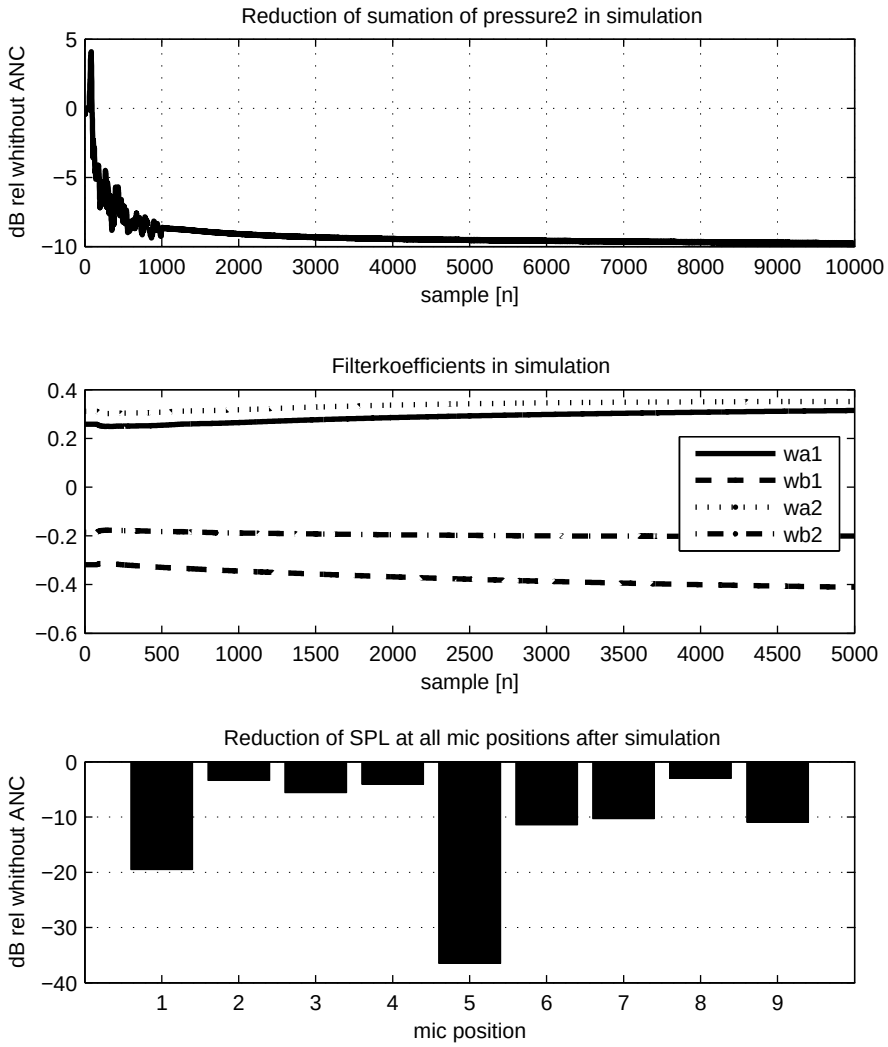

Figure 5.7. Simulation when frequency is 425Hz, particle velocity is "out of phase".

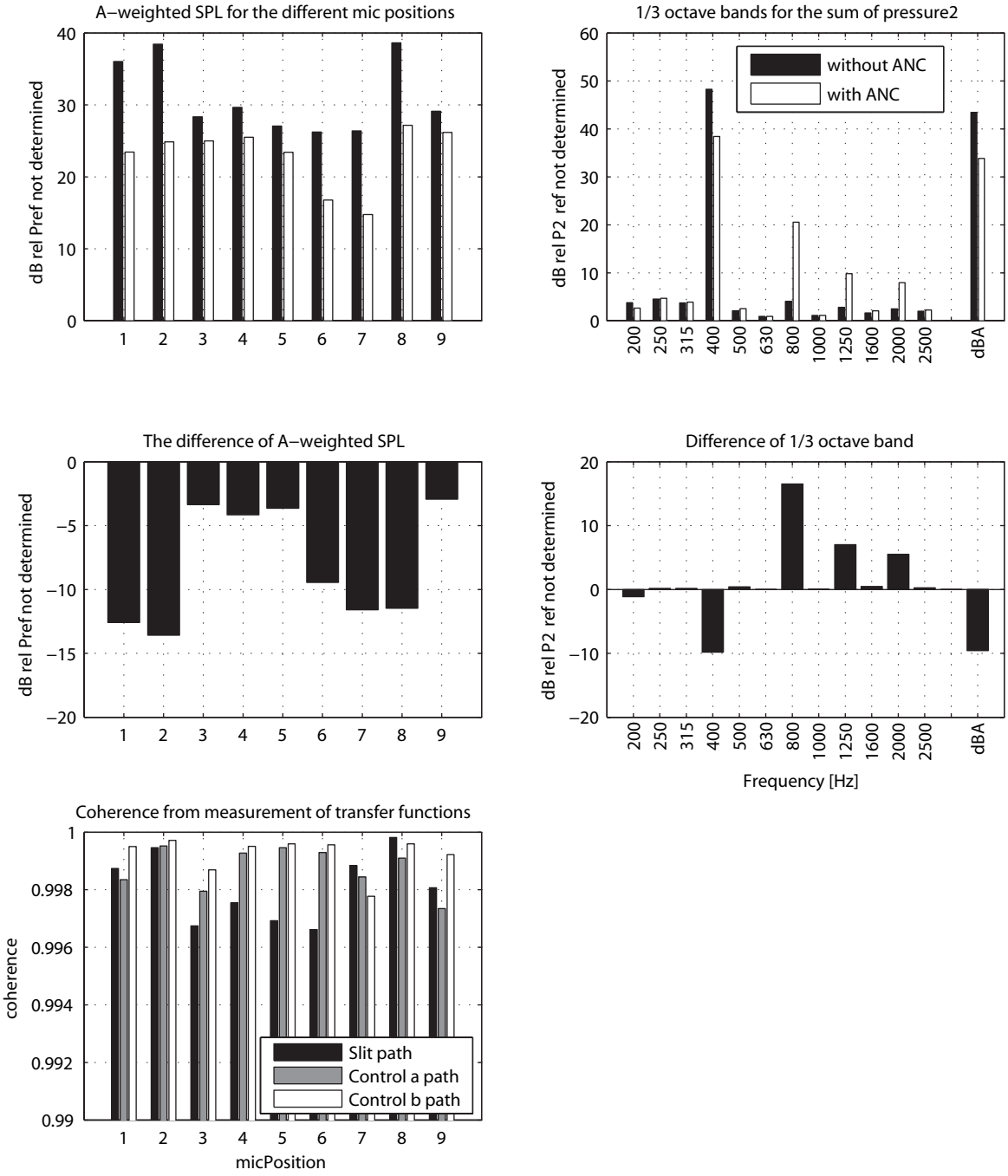

Figure 5.8. Experiment when frequency is 425Hz, particle velocity of slit is "out of phase".

5.5 900Hz, particle velocity "in phase"

In Figure 5.9 the time domain simulation can be seen when the particle velocity of the slit is in phase and has a frequency of 900 Hz. The results for the real experiment when the filter koefficients is imported from simulation can be seen in Figure 5.10.

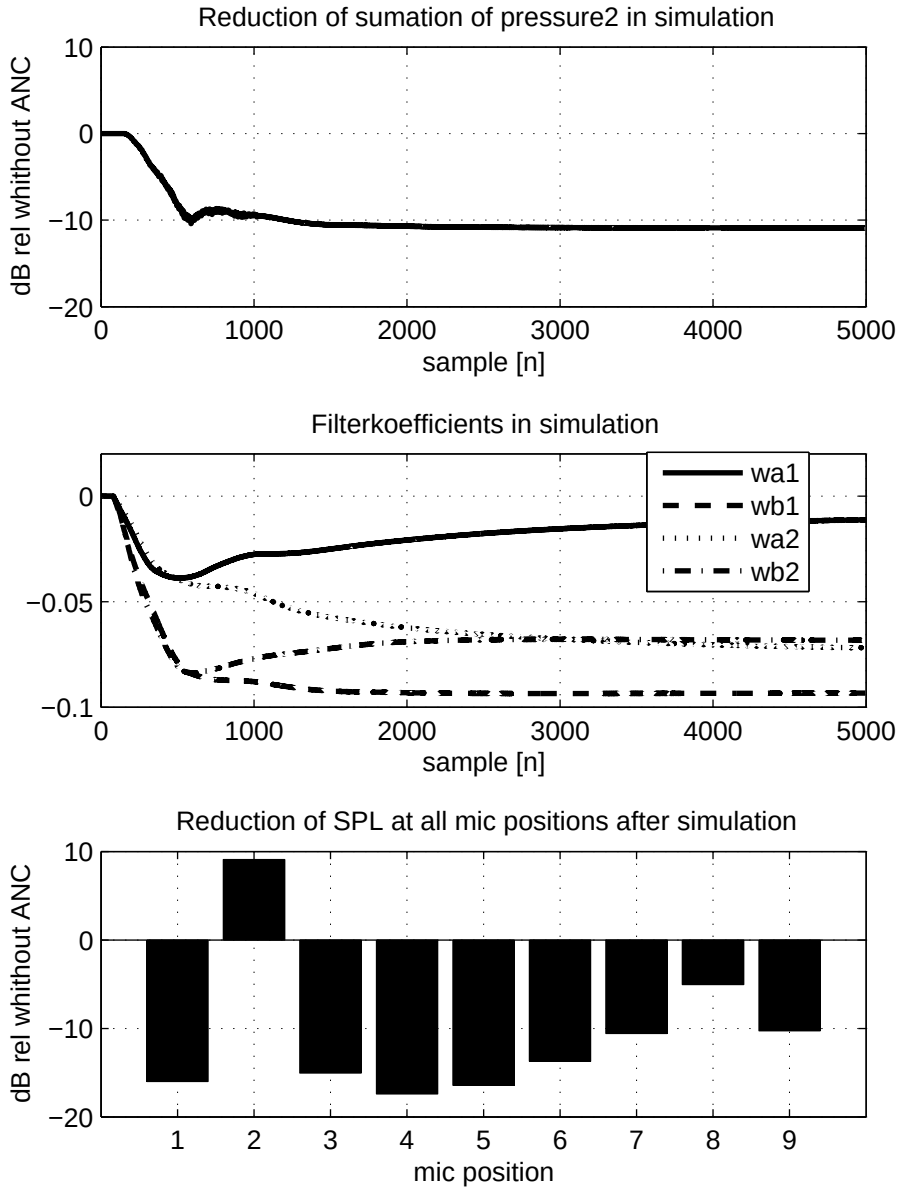

Figure 5.9. Simulation when frequency is 900Hz, particle velocity is "in phase".

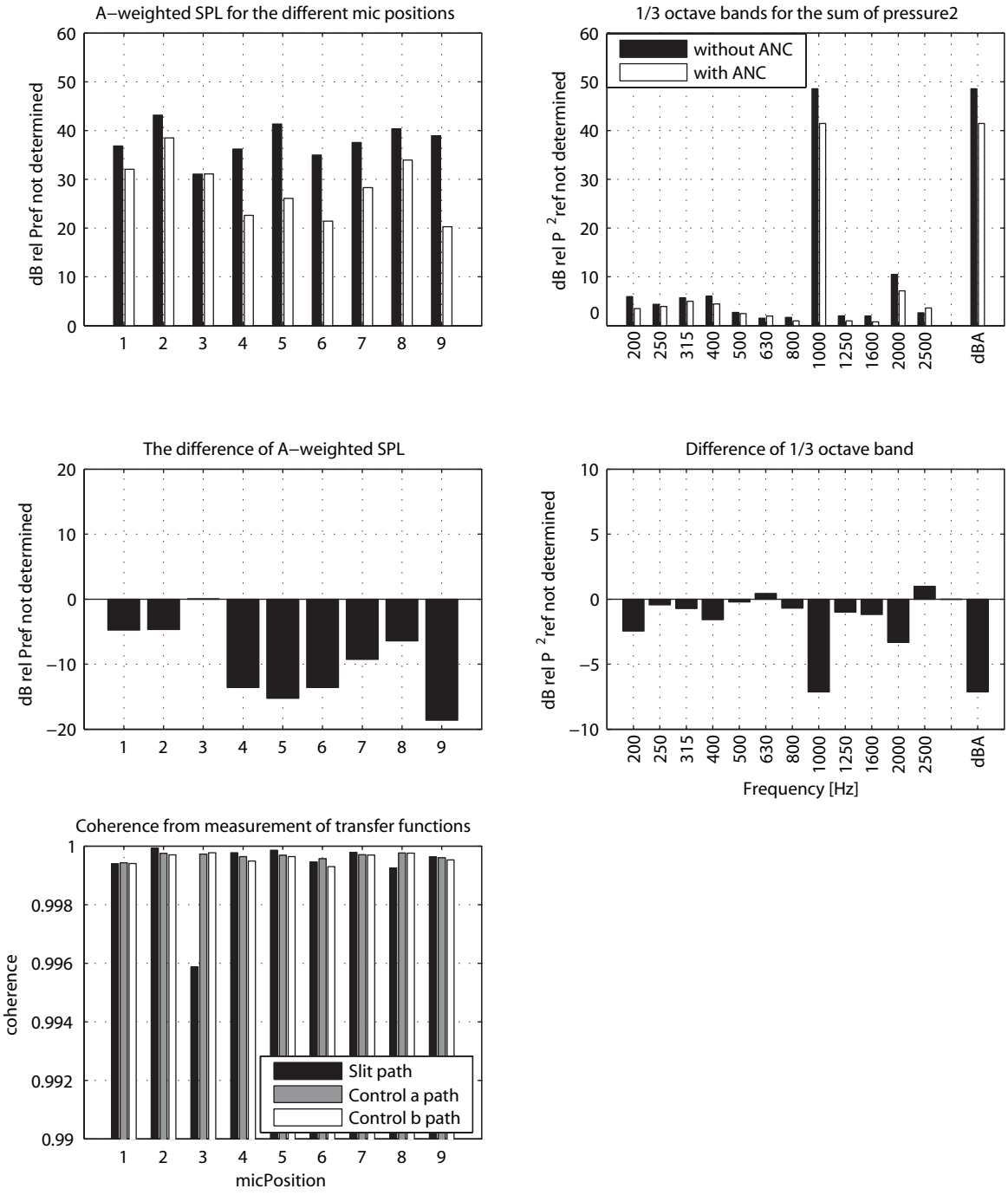

Figure 5.10. Experiment when frequency is 900Hz, particle velocity of slit is "in phase".

5.6 900Hz, particle velocity "out of phase"

In Figure 5.11 the time domain simulation can be seen when the particle velocity of the slit is out of phase and has a frequency of 900 Hz. The results for the real experiment when the filter koefficients is imported from simulation can be seen in Figure 5.12.

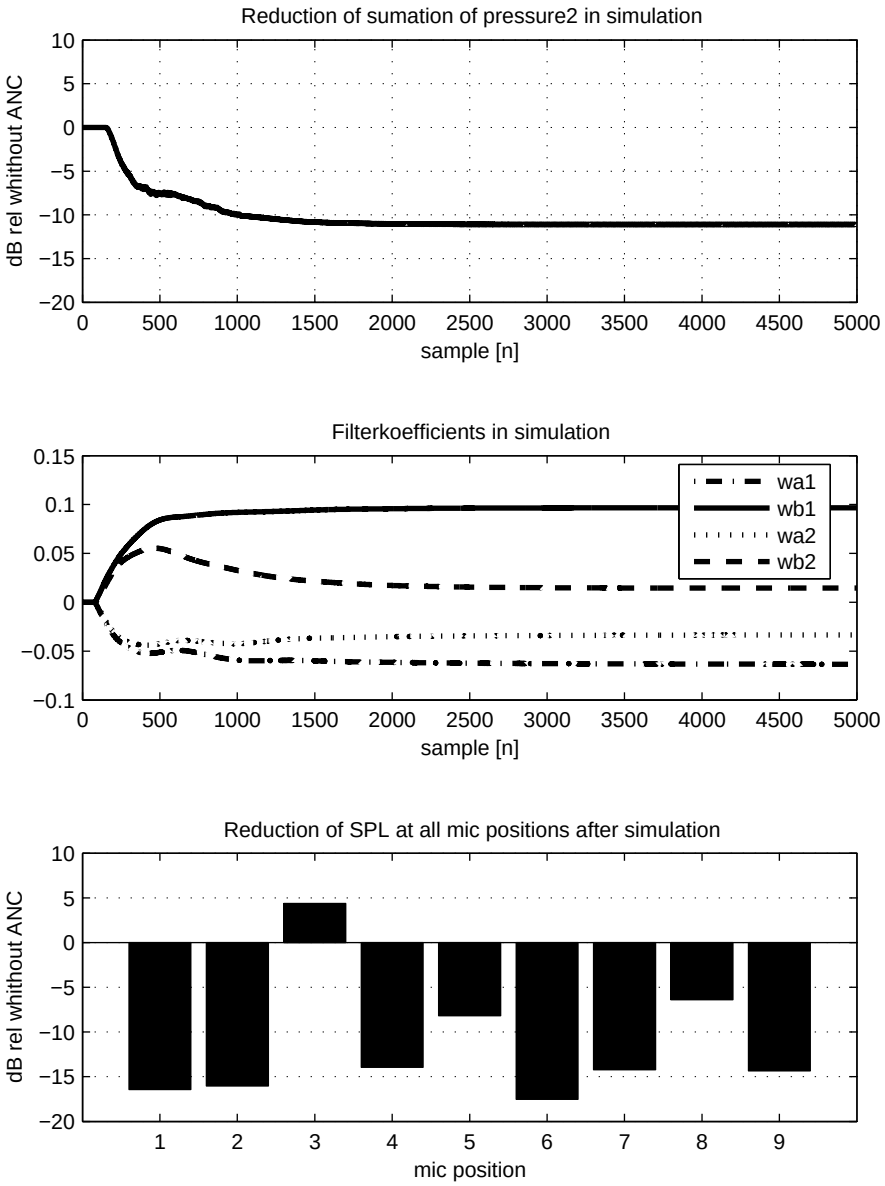

Figure 5.11. Simulation when frequency is 900Hz, particle velocity is "out of phase".

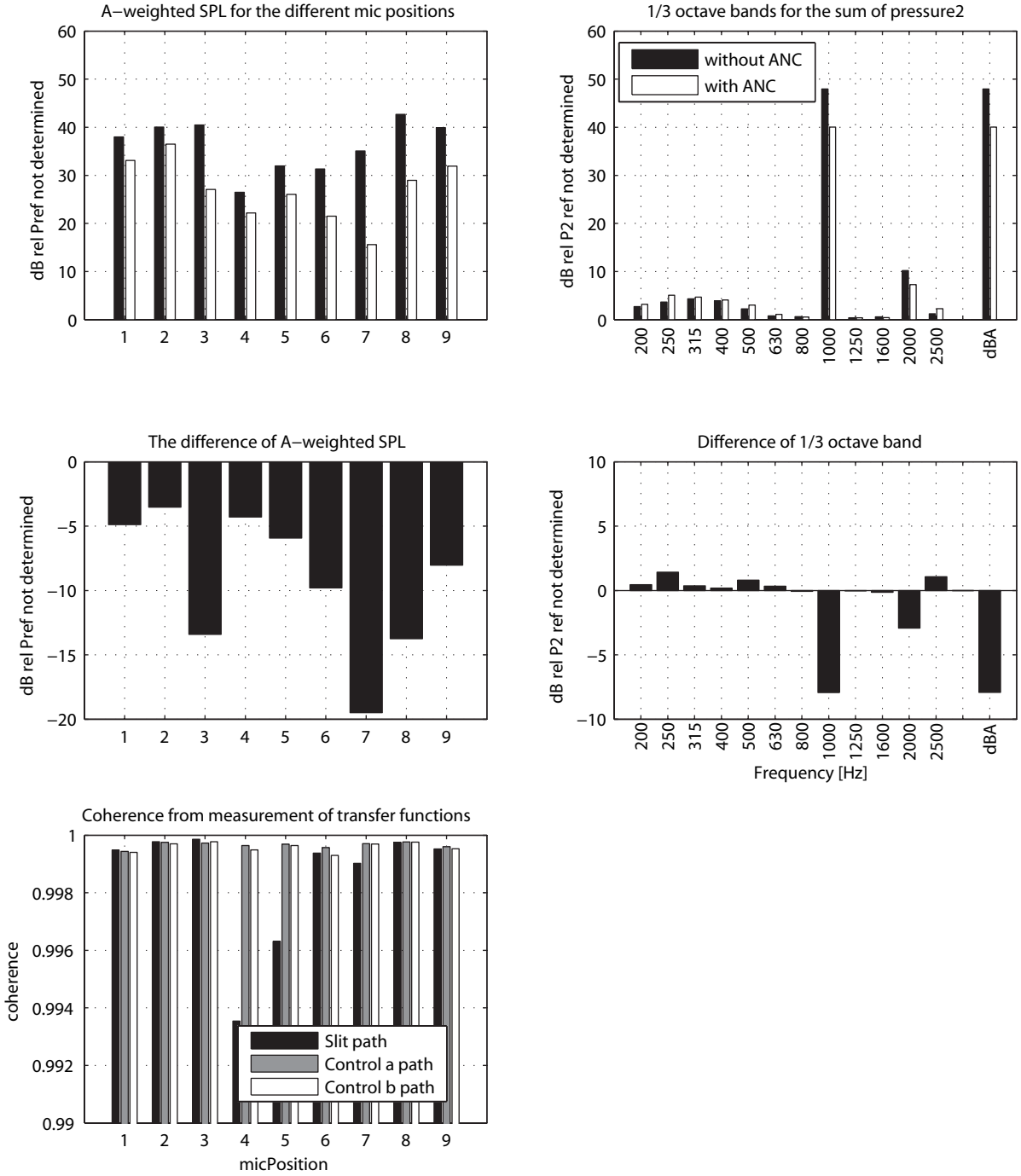

Figure 5.12. Experiment when frequency is 900Hz, particle velocity of slit is "out of phase".

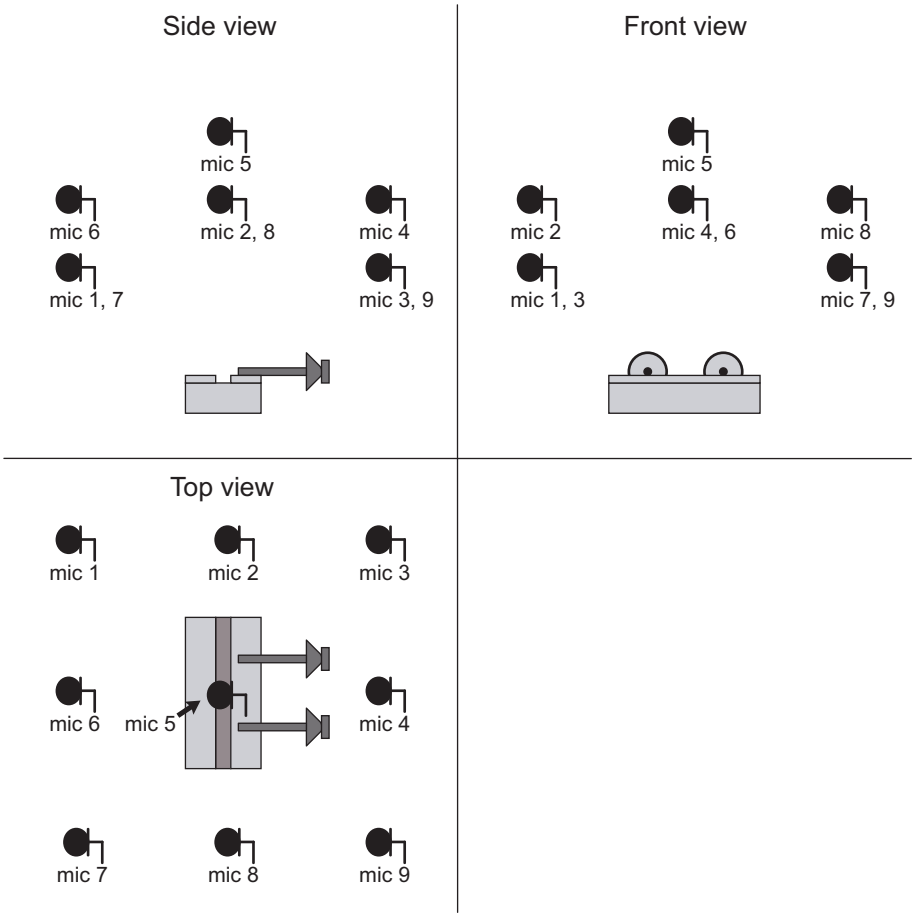

Figure 5.13. Illustration of the microphone positions in the experiment.

6 DISCUSSION

The results shows that in all six cases a reduction of the summation of the sound pressure squared is archived. This shows that the control algorithm worked as expected, otherwise there should be an increasement of the radiated sound power. The highest reduction is when the frequency from the slit is 425Hz and has a particle velocity that is in phase. The reduction is then approximately 13dBA (see Figure 5.6), which is a good result for the reduction of noise from a radiating slit. For the other "out of phase case" when the frequency is 425Hz the total reduction is almost 10dBA. When the frequency is changed to 400Hz the reduction is approximately 9dBA for the "in phase case" and 5dBA for the "out of phase case" (Figure 5.2 and 5.4). In Figure 5.2 and 5.4 you can also see that some of the overtones increases a lot. This depends on the choice of drivers as secondary sources. The problem with the drivers is to create low frequency sound pressures (Figure 4.7). If you look at the last frequency case 900Hz, the overtones is not increasing since the secondary sources is working in a frequency region that they are designed for. This means that they do not create any distortion. The total reduction for the 900Hz case is approximately 7dBA for the "in phase case" and 8dBA for the "out of phase case".
From all the experiment cases the coherence from the measurement of the transfer functions is at least 0.99. A coherence on 0.99 corresponds to a maximal reduction on 20 dB in this experiment (Elliott 2001). In all experiment cases the reduction is much lower (between 5-13dBA). Then if you look at the simulations you can see that the difference between maximum reduction and the reduction in the experiments is very small (Table 6.1). The conclusion from this is that the maximum

Table 6.1. Maximum reduction from simulations vs. experiments.

	Simulation	Experiment
400Hz, in phase	9dB	9dB
400Hz, in out of phase	6dB	5dB
425Hz, in phase	12dB	13dB
425Hz, in out of phase	10dB	10dB
900Hz, in phase	11dB	7dB
900Hz, in out of phase	11dB	8dB

reduction is limited by the simulation algorithm (XLMS-algorithm). But why is the redution not higher? From the theory part (section 3.1) a maximum reduction of 25dB was predicted. But in this part you assumed that the secondary sources was point sources, and in the real experiment the sources was drivers with a tube (Figure 4.6). Therefore you will not get a reduction of 25dB, but a reduction of around 10dB is still quite high reduction. In the cases when the frequencies are 900Hz the simulations predict that the reduction will be about 11dB, this is 3-4dB higher reduction than in the experiments. One thing that might contribute to this is when the ANC-system is switched on in the experimets, the total sound pressure will be so low that the background noise will influency the results.

By comparing the results from the three different frequency cases you can see that the reduction for 425Hz is about 4-5dB higher than for 400Hz. This might depend on the design of the tubes in the secondary sources. The tubes act like a quarter wave pipe and have a lot of resonances. If the frequency, that is to be controlled, is an anti resonace for the tube, the drivers for secondary sources will have problems to create the same sound pressure as the noise source creates.

7 CONCLUSION

From both theory and experiments in this thesis it has been shown that an active noise controll system will give a good result for the reduction of noise for this type of slit. This results that a reduction of the noise from an induction furnace can be achieved. If the noise from the slit part of the furnace can be controlled in same way as the slit in the experiment, a reduction on 6dB or more of the total radiated power from the furnace can presumably be archived. It has also been shown that the reduction of noise is independent of the type of the sound field from the slit. But the more complex the sound field is, the more secondary sources is needed to get a high reduction. The tube design of the secondary sources has also been shown that they are working, but can presumably be better by changing the design a bit. A big advanage with the implementation of an acitve noise control system on an induction furnace is that the reference signal can be measured from the electronic system in a induction furnace.

Before implementing this control system on a furnace one might examine some more things. One thing to look at is what happens when the slit is round instead of straight. Another question is the design of the secondary sources. There will probably be very different results of the noice reduction due to the resonances in the tube. At some frequencies, when the tube has an anti resonance, it is very hard to create the same sound pressure level from the secondary sources as from the noise source. Questions like, how long shall the tube be, what diameter is the best, is it better to have a tube that has another shape than straight (see Figure 7.1), would also be good to spend some time on. Another important thing to examine is the

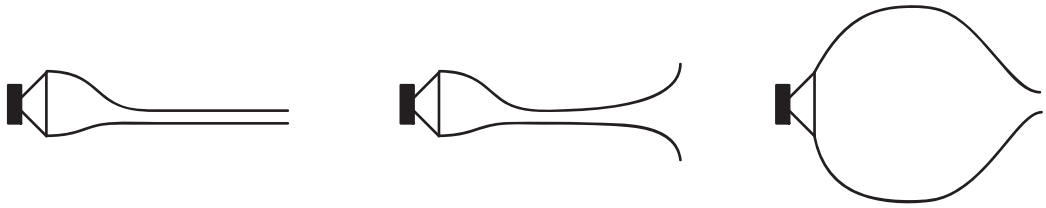

Figure 7.1. Suggestions on other tube shapes of the secondary sources.

implementation of the feed forward XLMS system in real time instead of the post processed approach that is used in this thesis. One advantage having the control system in real time is that the transfer functions does not need to be stationary. This real time system is very well suited for the induction furnace, because there can be big temperature changes that will result in different speed of sound, that will give different transfer functions.
After examining these questions it would be interesting to see if this system works on a real induction furnace.

Bibliography

D. H McQueen, H. Davidsson, C-G. Ekstrand G. Lundmark (1981). Reduction of noise from induction furnaces. i. air borne sound. *Sandinavian Journal of Metallurgy*, (10), 211–215.

Determination of sound power levels of noise sources using sound intensity (1996). ISO 9614-2.

Dötsch, E. (1994). Den tysta högpresterande induktionsdegelugnen för mellanfrekvens. *ABB tidning*, (4), 15–22.

Elektrougnar och induktiva omrörare (1969). ASEA. Västerårs.

Elliott, S.J. (2001). *Signal Processing for Active Control*. 1st edn. Academic press. London.

Fahy, F. J. (1989). *Sound Intensity*. 1st edn. Elsevier Science Publishing CO. New York.

Hayes, Monson H. (1996). *Statistical Signal Processing and Modeling*. 1st edn. John Wiley and Sons, Inc. New York.

Kleiner, Mendel (1991). *Audioteknik och Akustik*. 2nd edn. Teknisk Akustik, CTH. Gothenburg.

McQueen, D. H (1982*a*). Reduction of noise from induction furnaces. ii. noise generation mechanism. *Sandinavian Journal of Metallurgy*, (11), 173–178.

McQueen, D. H (1982*b*). Reduction of noise from induction furnaces. iii. evaluation. *Sandinavian Journal of Metallurgy*, (11), 309–312.

P. A. Nelson, A. R. D. Curtis, S. J. Elliott A. J. Bullmore (1987). The minimum power output of free field point sources and the active control of sound. *Journal of Sound and Vibration*, **116**(3), 397–414.

P.A. Nelson, S.J. Elliott (1992). *Active Control of Sound*. 1st edn. Academic press. London.

Snyder, Scott D. (2000). *Active Noise Control Primer*. 1st edn. Springer-Verlag. New York.

T. Bauer, G. Henneberger (1999). Three-dimensional calculation and optimization of the acoustic field of an induction furnace caused by electromagnetic forces. *IEEE Transations on magnetics*, **35**(3), 1598–1601.

T. Bauer, J. Gschwilm, G. Henneberger (2001). Comparison of 3-d coupled calculations and measurements concerning the structural-dynamic behaviour of induction furnaces excited by electromagnetic forces. *IEEE Transations on magnetics*, **37**(5), 3433–3436.

T. Bauer, W. Mai, G. Henneberger (2000). Improved 3d coupled calculations of the structural-dynamic behavior of induction furnaces excited by electromagnetic forces using adaptive algorithms. *IEEE Transations on magnetics*, **36**(4), 1565–1568.

Appendix A

Notation

app:Notation

Abbreviations

PSD	power spectrum density
FFT	fast fourier transform
FRF	frequency response function
TF	transfer function

Capital Letters

J	cost function
W	sound power (*watt*)
$\mathbf{G}$	transfer function of the plant response
$\mathbf{W}$	controller transfer function
$\mathbf{Z}$	impedance matrix

Small Letters

c	speed of sound $[\frac{m}{s}]$
d	disturbance signal
e	error signal
f	frequency $[Hz]$
k	wave number $[\frac{rad}{m}]$
p	sound pressure $[Pa]$
$\mathbf{p}$	vector of sound pressures $[Pa]$
q	volym velocity $[\frac{m^3}{s}]$
$\mathbf{q}$	vector of particle velocities $[\frac{m}{s}]$
t	time $[s]$
v	particle velocity $[\frac{m}{s}]$
$\mathbf{w}$	filter coefficients
x	reference signal
y	output signal from filter
z	impedance

Greek Letters

α	convergence coefficient for the LMS algoritm
λ	wave length $[m]$
ω	angular frequency $[\frac{rad}{sec}]$
ρ_0	density of air $[\frac{kg}{m^3}]$

Appendix B

Post processing in Bullerby software

app:postProcessing

```
global AGxy Xblocks;
if N==1
  clear X1 Sx Hxy Rxy
end

% Initial setup
% ********************************************************************
% Compute # of alias protected frequency components
L = size(X,1)/2.56 + 1
dF = Span/(L-1); % Frequncy resolution
% NB=number of frequency components, M=number of active channels
[NB,M]=size(X);
t=(1:length(X))/NB/dF;  % Building time axis
f=(0:NB-1)*dF; % Build frequency axis

% Windowing and calibration
% ********************************************************************
wind=hanning(NB); % Hanning window
% Compenstion factor for the energy lost when applying the window
w_fact=sqrt(sum(wind.^2)/NB);
% Windowing and compensation on the time signal
X1=X.*wind(:,ones(1,M))/w_fact;


for m = 1:M
   Xcalib(1,:,m) = X(:,m).*C(m); %%karls fix
   % Calibration accoriding to the factors specified in Bullerby
   X1(:,m) = X1(:,m).*C(m);
end
```

```
% sparar hela tidsignalen dvs summerar upp bufferterna
if N==1
  Xblocks = Xcalib;
else
  Xblocks = [Xblocks ;Xcalib];
end
%Xblocks(:,:,N) =Xcalib;


% ************************************************************************
% Fourier transform
% ************************************************************************
% fft has to be divided by block size to get the right
S = fft(X1)/NB;
% scale for a double sided amplitude spectrum

Sx=S(:,:); %

% ************************************************************************
% Compute autospectra and cross spectra
% ************************************************************************

% Calculating spectra
for i1=1:M
for i2=1:M
  Gxy(:,i1,i2)=conj(Sx(:,i1)).*Sx(:,i2);
end
end

% Averaging spectra
if N==1
  AGxy = zeros(L-1,M,M);
  AGxy = Gxy;
else
   AGxy = AGxy - (AGxy - Gxy)/N;
end

% Calculating transfer functions
for i1=1:M
   for i2=1:M
      % H1 estimator
      Hxy(:,i1,i2)  = AGxy(:,i1,i2) ./ AGxy(:,i1,i1);
      % H2 estimator
      %Hxy(:,i1,i2)  = AGxy(:,i2,i2) ./ AGxy(:,i2,i1);
end
end
```

```
% Calculating coherence functions
for i1=1:M
for i2=1:M
      Rxy(:,i1,i2)=AGxy(:,i1,i2).*AGxy(:,i2,i1)
       ./AGxy(:,i1,i1)./AGxy(:,i2,i2);
end
end


% ************************************************************************
% Presentation
% ************************************************************************

% setting up the collours used for plotting
collar=['rbgkmcyrbgkmcyrbgkmcy'];

if N==1
close all
figure(1)
h1=gcf;
set(h1,'position',[140 330 400 266]);
figure(2)
h2=gcf;
set(h2,'position',[550 330 400 266])
figure(3)
h3=gcf;
set(h3,'position',[140 59 400 266])
figure(4)
h4=gcf;
set(h4,'position',[550 59 400 266])
end

if M==1  % if only one channel (no transfer or coherence)
   figure(1)
   plot(t,X)
   title('Time signal')

   % ploting the single sided version of the spectrum
   figure(2)
   plot(f(1:L),10*log10(abs([AGxy(1,1,1); 2^2*AGxy(2:L,1,1)])))
   title('Auto spectrum')

else % if more than one channel
   for nm=1:M;
      figure(1)
```

```
      eval(['plot(t,X(:,nm),''',collar(nm),''')']) % time signals
      hold on

       % auto spectra
      figure(2)
      eval(['plot(f(1:L),10*log10(abs([AGxy(1,nm,nm);
       2^2*AGxy(2:L,nm,nm)])),''',collar(nm),''')'])
      hold on

      % transfer functions
      figure(3)
      if nm>1
      eval(['plot(f(1:L),20*log10(abs([Hxy(1,1,nm);
        Hxy(2:L,1,nm)])),''',collar(nm),''')'])
      hold on
      end

      figure(4)
      if nm>1
      % coherence functions
      eval(['plot(f(1:L),Rxy(1:L,1,nm),''',collar(nm),''')'])
      hold on
      end

   end

   % setting up a legend text for the time signal window
leg_text=['''ch 1'''];
for nm=2:M;
    leg_text=[leg_text,',''ch ',num2str(nm),''''']
end

   figure(3)
   hold off
   title('Transfer function')
   drawnow

   figure(4)
   hold off
   title('Coherence function')
   drawnow

   figure(1)
   hold off
   title('Time signal')
   eval(['legend(',leg_text,')'])
```

```
   drawnow

   figure(2)
   hold off
  title('Auto spectrum')
   drawnow
end
% ************************************************************************
% End of program
% ************************************************************************
```